



VYSOKÉ UČENÍ TECHNICKÉ V BRNĚ
BRNO UNIVERSITY OF TECHNOLOGY



FAKULTA STROJNÍHO INŽENÝRSTVÍ
LETECKÝ ÚSTAV

FACULTY OF MECHANICAL ENGINEERING
INSTITUTE OF AEROSPACE ENGINEERING

COMPARISON OF PANEL CODES FOR AERODYNAMIC ANALYSIS OF AIRFOILS

POROVNÁNÍ MOŽNOSTÍ PANELOVÝCH METOD PRO AERODYNAMICKOU ANALÝZU PROFILŮ

BAKALÁŘSKÁ PRÁCE
BACHELOR'S THESIS

AUTOR PRÁCE
AUTHOR

ADAM BILČÍK

VEDOUCÍ PRÁCE
SUPERVISOR

Ing. ROBERT POPELA, Ph.D.

BRNO 2014

Vysoké učení technické v Brně, Fakulta strojního inženýrství

Letecký ústav

Akademický rok: 2013/2014

ZADÁNÍ BAKALÁŘSKÉ PRÁCE

student(ka): Adam Bilčík

který/která studuje v bakalářském studijním programu

obor: **Strojní inženýrství (2301R016)**

Ředitel ústavu Vám v souladu se zákonem č.111/1998 o vysokých školách a se Studijním a zkušebním řádem VUT v Brně určuje následující téma bakalářské práce:

Porovnání možností panelových metod pro aerodynamickou analýzu profilů

v anglickém jazyce:

Comparison of panel codes for aerodynamic analysis of airfoils

Stručná charakteristika problematiky úkolu:

Cílem práce je seznámení studenta se zcela základním principem řešení úloh obtékání profilů pomocí panelové metody a vytvoření přehledu v současné době používaných implementací. Dále porovnání možností jednotlivých metod a programů a srovnání z hlediska omezení a použití na typické úlohy.

Cíle bakalářské práce:

Vytvoření přehledu v současné době používaných implementací panelových metod pro aerodynamické výpočty charakteristik 2D profilů. Základní popis principu panelové metody, porovnání jednotlivých implementací a zhodnocení jejich možností (přesnost, aplikovatelnost) na typické úlohy.

Seznam odborné literatury:

- [1] Kuethe, A., Chow, Ch.-Y., Foundations of Aerodynamics - Bases of Aerodynamic Design, John Wiley and Sons, ISBN 0-471-12919-4
- [2] Plotkin, A., Katz, J., Low-Speed Aerodynamics (Cambridge Aerospace Series), Cambridge University Press, ISBN 978-0521665520
- [3] Drela, M., Youngren H., XFOIL 6.9 User Primer, http://web.mit.edu/drela/Public/web/xfoil/xfoil_doc.txt

Vedoucí bakalářské práce: Ing. Robert Popela, Ph.D.

Termín odevzdání bakalářské práce je stanoven časovým plánem akademického roku 2013/2014.

V Brně, dne

L.S.

doc. Ing. Jaroslav Juračka, Ph.D.
Ředitel ústavu

doc. Ing. Jaroslav Katolický, Ph.D.
Děkan fakulty

ABSTRACT

The purpose of this study is to create an overview of currently the most used panel codes for computation of aerodynamic characteristics of 2D airfoils. Description of the basic principles of panel code, comparison of various implementation and evaluation (accuracy, applicability) for typical tasks. In this thesis there were used three different panel codes: Xfoil, JavaFoil and XFLR5. Thesis was enriched by measurement in wind tunnel.

ABSTRAKT

Cieľom tejto práce bolo vytvorenie prehľadu v súčasnosti používaných implementácií panelových metód pre aerodynamické výpočty charakteristík 2D profilov. Základný popis princípu panelovej metódy, porovnanie jednotlivých implementácií a zhodnotenie ich možností (presnosť, aplikovateľnosť) na typické úlohy. V práci boli použité tri rôzne panelové programy: Xfoil, JavaFoil a XFLR5. Práca bola obohatená o meranie v aerodynamickom tuneli.

KEYWORDS

Panel Method, NACA 0012, Airfoil, XFOIL, JavaFoil, XFLR5, Wind tunnel, Lift coefficient, Drag coefficient, Pitching moment coefficient, Polar curve

KLÚČOVÉ SLOVÁ

Panelová metóda, NACA 0012, profil krídla, XFOIL, JavaFoil, XFLR5, Aerodynamický tunel, súčiniteľ vztlaku, súčiniteľ odporu, koeficient klopivého momentu, aerodynamická polára

BIBLIOGRAPHIC CITATION

BILČÍK, Adam. *Comparison of panel codes for aerodynamic analysis of airfoils*. Brno: Brno University of Technology, Faculty of mechanical engineering, 2014. 42 p. Supervised by Ing. Robert Popela, Ph.D.

DECLARATION OF AUTHENTICITY

I, Adam Bilčík, declare that I prepared this bachelor's thesis independently and disclosed all sources and literature.

28. 5. 2014

.....
Adam Bilčík

ACKNOWLEDGEMENT

At this point I would like to thank my bachelor's thesis supervisor Ing. Robert Popela, Ph.D. for his continuing support, guidance, patient and valuable tips during this challenging thesis. Also I want to express my thanks to Ing. Jan Pejchar who helped me with the realization of wind tunnel measurement and with analysis of the results. I am looking forward to my master studies at the Institute of the Aerospace Engineering.

CONTENT

INTRODUCTION	10
1 AERODYNAMIC CHARACTERISTICS OF AIRFOILS.....	11
1.1 PRESSURE DISTRIBUTION ON AN AIRFOIL	12
1.2 PITCHING MOMENT	14
1.3 WAKE GENERATED BY THE AIRFOIL.....	15
2 PANEL CODES.....	16
2.1 DEVELOPMENT OF PANEL CODES	17
2.2 XFOIL v6.94	18
2.2.1 <i>User's Interface</i>	18
2.3 JAVAFOIL v2.21	21
2.3.1 <i>User's Interface</i>	21
2.4 XFLR5 v4.17	24
2.4.1 <i>User's Interface</i>	24
3 WIND TUNNEL MEASUREMENT	26
3.1 THE WIND TUNNEL	26
3.2 TEST SET UP.....	27
3.3 THE MEASUREMENT	28
4 NACA REPORT.....	30
5 COMAPARISON OF RESULTS.....	32
5.1 LIFT CURVE	34
5.2 PITCHING MOMENT CURVE.....	35
5.3 POLAR CURVE.....	36
5.4 EVALUATION OF RESULTS	37
CONCLUSION	38
BIBLIOGRAPHY	39
LIST OF SYMBOLS	40
LIST OF FIGURES	41
CONTENTS OF THE ENCLOSED CD.....	42

INTRODUCTION

Throughout the development of flight, every aircraft has required some kind of device which produce lift. Most of the aircrafts use wings for producing lift. Wing design is constantly improving by the time of the first airplane - the Wright Flyer. There have been many organisations and aircraft producers which investigated aerodynamic characteristics of airfoils to reach better flight characteristics. Their research had various forms from using of wind tunnels widely in the past to the computation of numerical panel codes. In this thesis it is focus on panel methods.

With the advent of computers, these methods have been used increasingly to complement wind-tunnel tests. Today, computing costs are so low that a complete potential-flow and boundary-layer analysis of an airfoil costs considerably less than one per cent of the equivalent wind tunnel test. Accordingly, the tendency today is toward more and more commonly applicable computer codes. These codes reduce the amount of required wind tunnel testing and allow airfoils to be tailored to each specific application. [9]

Chapter 1 discusses the aerodynamic characteristics of an airfoil. There is a basic description of geometrical variables of an airfoil, pressure distribution over an airfoil, pitching moment of the airfoil and drag generated by airfoil. Properties in this chapter are valid for the symmetrical airfoil.

In chapter 2, the panel codes are presented. In section 2.1, there is brief insight to the history of its development and list of some currently most used panel codes. There is also detailed look at three different panel codes used in this thesis.

Chapter 3 is focused on added wind tunnel measurement performed in facilities of Institute of Aerospace Engineering at Brno University of Technology.

Chapter 4 describes the role of NACA organization and there is a report for an airfoil used in this thesis which is compared with results from wind tunnel measurement and panel codes.

1 AERODYNAMIC CHARACTERISTICS OF AIRFOILS

Theory in this chapter is detailed explained in the book: Foundations of Aerodynamics – Bases of Aerodynamic Design. [1]

The airfoils are composed of a thickness envelope wrapped around a mean camber line in the manner shown in Figure 1.1. The mean camber line lies in the middle of upper and lower surface of the airfoil and intersects the chord line at the leading and trailing edges.

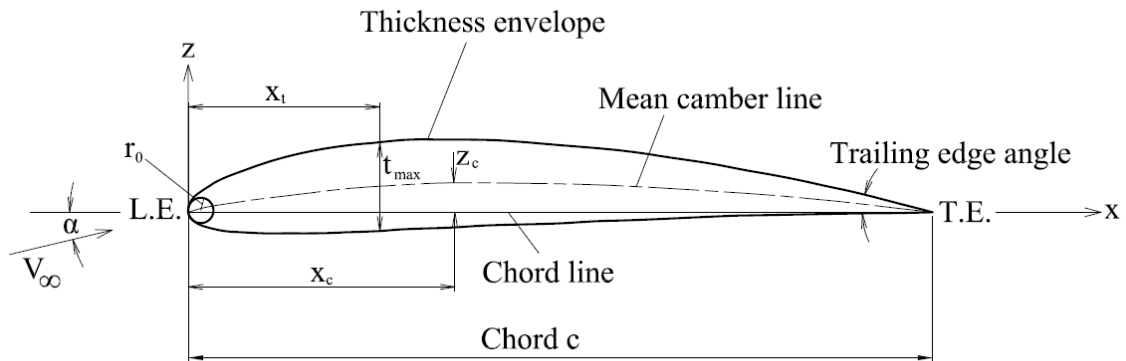


Fig. 1.1. Airfoil geometrical variables

The geometric angle of attack α is defined as the angle between the flight path and the chord line of the airfoil, as depicted in Fig. 1.1. The geometrical variables include the maximum camber z_c of the mean camber line and its distance x_c behind the leading edge, maximum thickness t_{max} and its distance x_t behind the leading edge, the radius of curvature r_0 of the surface at the leading edge and trailing edge angle between the upper and lower surfaces at the trailing edge.

Properties of the airfoil described in this chapter are valid for the symmetrical airfoil in which the chord line and mean camber line are coincident.

1.1 Pressure distribution on an airfoil

Bernoulli's equation is expressed, with hydrostatic pressure term omitted for aerodynamic analyses as

$$p + \frac{1}{2}\rho V^2 = p_0$$

It signifies that, in a steady, incompressible, and irrotational flow of gaseous fluid, the sum of the static and dynamic pressure (or the total pressure p_0) remains a constant. Since p_0 is the static pressure at a stagnation point, it is also called the *stagnation pressure* of the flow.

In practical measurements on flow around bodies, data are generally presented in terms of the *pressure coefficient*, C_p . To define C_p , we assume irrotational flow so that p_0 is constant everywhere and we identify p_∞ and V_∞ as values far from the body:

$$p + \frac{1}{2}\rho V^2 = p_\infty + \frac{1}{2}\rho V_\infty^2$$

Using a standard abbreviation, $q = \frac{1}{2}\rho V^2$, we define the pressure coefficient for incompressible flows:

$$C_p = \frac{p - p_\infty}{q_\infty} = 1 - \left(\frac{V}{V_\infty}\right)^2$$

where $q_\infty = \frac{1}{2}\rho V_\infty^2$ and p_∞ is the barometric pressure. Then, in an incompressible flow, $C_p = 1$ at a stagnation point where $V = 0$, and $C_p = 0$ far from the body where $V = V_\infty$.

The lift per unit area at a given location is numerically equal to the difference in pressure between the upper and lower surfaces at the point. Figure 1.2 shows chordwise plots of the pressure coefficients for the lower and upper surfaces on NACA 0012 airfoil at an angle of attack $\alpha = 6^\circ$, and

$$\Delta C_p = C_{pL} - C_{pU} = \frac{\Delta p}{q_\infty}$$

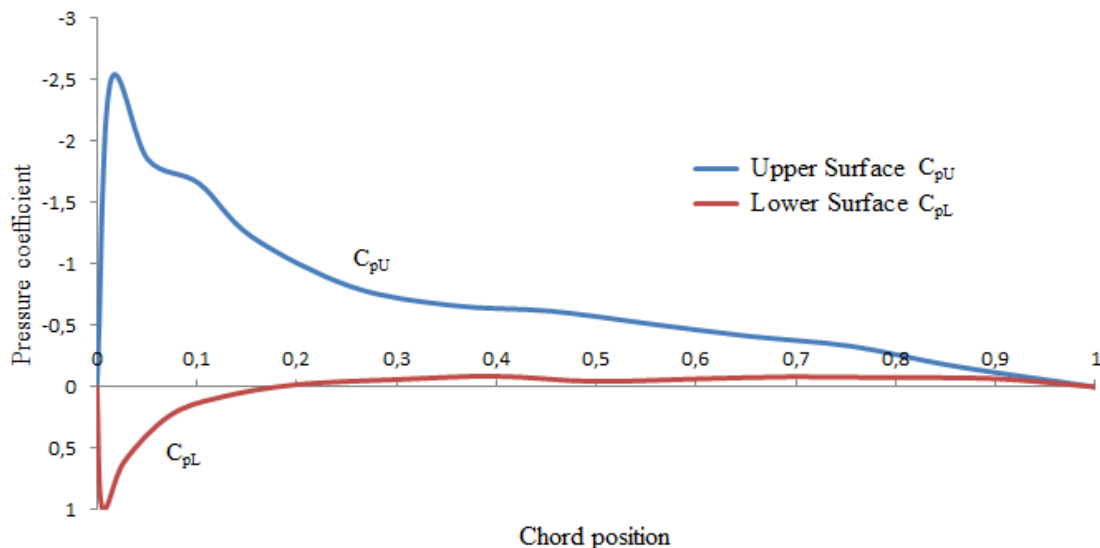


Fig. 1.2. Distribution of pressure coefficient on NACA 0012 airfoil at $\alpha = 6^\circ$

The lift per unit span L' :

$$L' = \int_0^c \Delta p x dx$$

The appropriate dimensionless parameter is the *sectional lift coefficient* defined by

$$c_l = \frac{L'}{q_\infty c}$$

which leads to result:

$$c_l = 2\pi\alpha \equiv m_0\alpha$$

where m_0 is the slope of the c_l versus α curve and the angle α is in radians. It's indicates in theory that the sectional lift coefficient for a symmetrical airfoil is directly proportional to the geometric angle of attack. Further, when the geometric angle of attack is zero, the lift coefficient is zero as is shown on Figure 1.3.

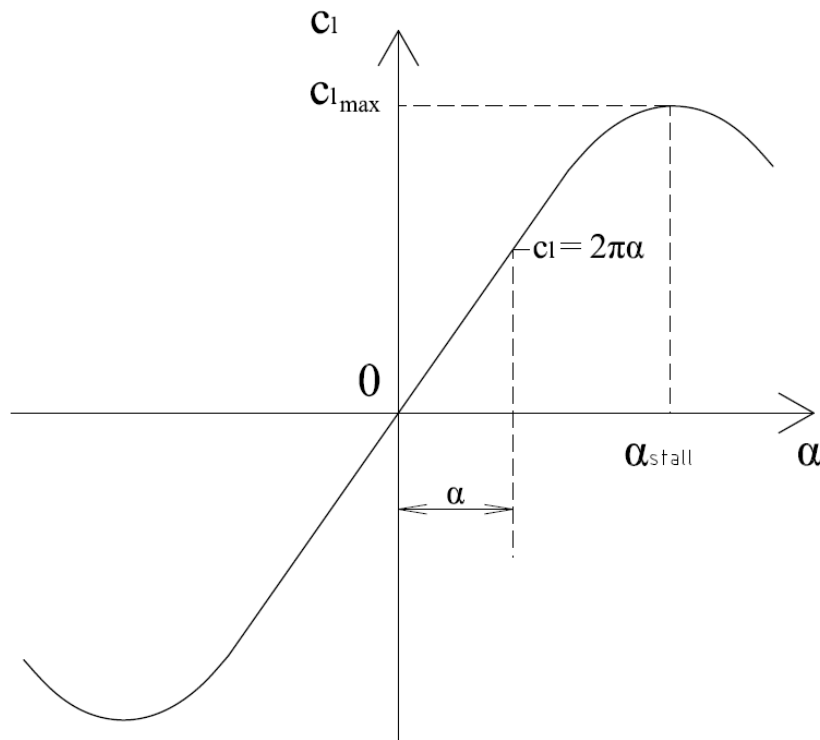


Fig. 1.3. c_l versus α curve for symmetrical airfoil

The geometrical angle of attack with maximal sectional lift coefficient $c_{l_{max}}$ is called α_{stall} .

1.2 Pitching moment

The moment of the lift about the leading edge of the airfoil is given by

$$M'_{LE} = - \int_0^c \Delta p x dx$$

A stalling moment is taken as positive (clockwise in Figure 1.4). By use of previously stated equations we define a *sectional moment coefficient*:

$$c_{m_{LE}} = \frac{M'_{LE}}{q_{\infty} c^2} = - \frac{\pi \alpha}{2}$$

Or in terms of the lift coefficient,

$$c_{m_{LE}} = - \frac{c_l}{4}$$

The *centre of pressure* on the airfoil is the point of action of the resultant pressure force (or the lift), whose chordwise location x_{cp} is determined from the requirement that, about any given point, the moment caused by the lift must be the same as that caused by the distributed pressure on the airfoil. Taking the leading edge as the point about which moments are computed:

$$L' x_{CP} = -M'_{LE}$$

and with the use of the previous equations we have:

$$x_{CP} = \frac{c}{4}$$

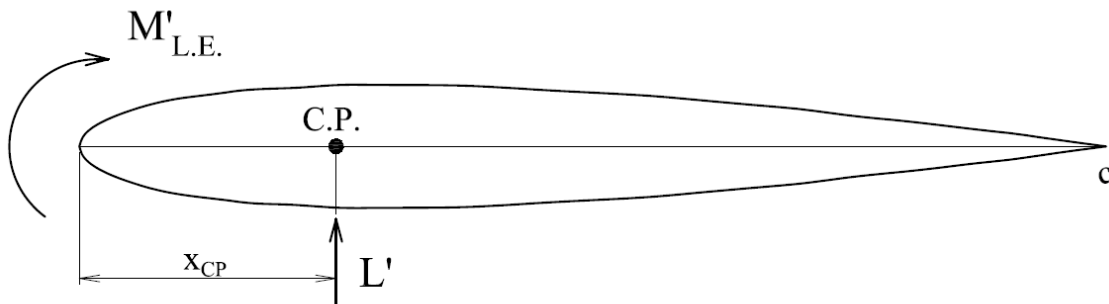


Fig. 1.4. Moment about leading edge

1.3 Wake generated by the airfoil

Wake is the region of disturbed flow downstream of a solid body moving through a fluid, caused by the flow of the fluid around the body. [11] In the wake region, the velocity is less than the upstream value, as illustrated by the profile at the right part of the Figure 1.5.

Conservation of mass for flow through the stream tube requires that

$$\rho V_1 dy_1 = \rho V_2 dy_2$$

and

$$D' = \int \rho V_2 (V_1 - V_2) dy_2$$

where $\rho V_2 dy_2$ is the mass of fluid leaving dy_2 per unit time, and during its flow around the body, its velocity is decreased from V_1 to V_2 . The integrand is therefore the momentum lost by the fluid leaving the control volume through dy_2 per unit time. In the absence of pressure forces on the control surface, the integral is the loss of momentum suffered by the fluid passing through the downstream plane per unit time, which, by the momentum theorem, is exactly equal to the drag per unit length of the airfoil. Knowing that, the *drag coefficient* can be expressed as:

$$c_d = \frac{2D}{\rho V_1^2 c} = \frac{2}{c V_1^2} \int_T^B V_2 (V_1 - V_2) d\frac{y}{c}$$

where, V_1 is the velocity of the upstream, V_2 is the wake velocity, y is the transvers position at which the wake velocity is being measured, c is the chord length of the airfoil, T is the top of the transverse range, B is the bottom of the transverse range of the wake region.

Drag generated by the body (or an airfoil) can be divided to the 2 components:

- a) Friction drag component C_{D_f}
- b) Pressure drag component C_{D_p}

$$C_D = C_{D_f} + C_{D_p}$$

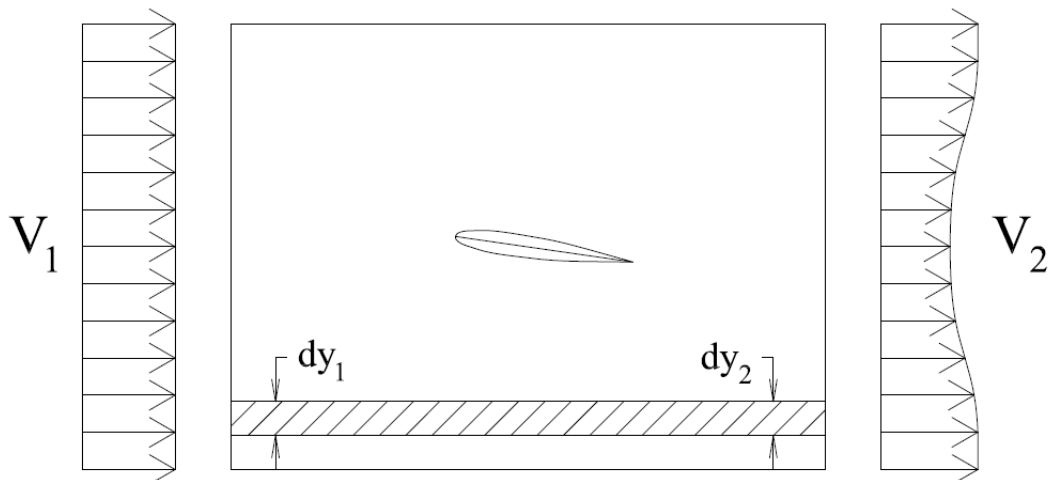


Fig. 1.5. Drag of an airfoil from wake measurements

2 PANEL CODES

In fluid dynamics, panel codes are used to determine the fluid velocity, and subsequently the pressure distribution, on an object. This may be a simple two-dimensional object, such as a circle or wing, or it may be a three-dimensional vehicle. A series of singularities as sources, sinks, vortex points and doublets are used to model the panels and wakes. These codes may be valid at subsonic and supersonic speeds. [7]

The geometry of the airfoil (or any other object) is divided into straight, individual panels shown on Figure 2.1. Mathematically, each panel induces a (yet unknown) velocity on itself and also on the remaining panels. This velocity can be expressed by relatively simple equations, which contain geometric relations like distances and angles between the panels only. All these influences are collected in a matrix and, additionally, a flow condition is defined on the surface, which must be satisfied by the induced velocities. This boundary condition is the requirement that the flow does not pass through the airfoil, but flows tangential along the surface. Together with the onset flow direction, a system of linear equations can be composed and solved for the unknown panel velocities. [4]

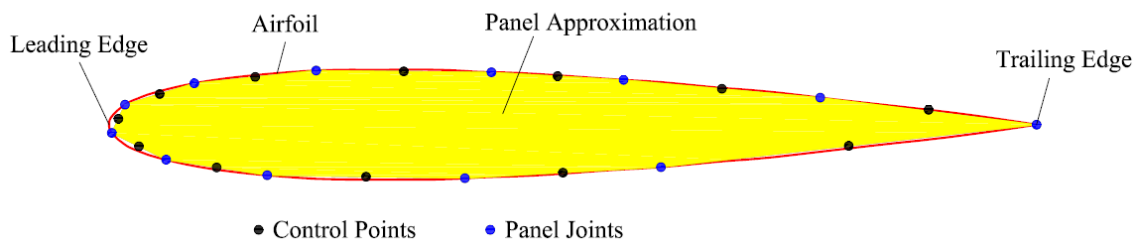


Fig. 2.1. Panel approximation to an airfoil

Each panel is defined by its two end points (panel joints) and by the control point, located at the panel centre, where the boundary condition will be applied.

The higher number of panels leads to more accurate results.

2.1 Development of Panel Codes

The computation of the aerodynamic characteristics of aircraft configurations has been carried out by panel methods since the mid 1960's, following the pioneering work of Hess & Smith of Douglas Aircraft in 1967 and Rubbert & Saaris of Boeing Aircraft in 1968. But even before the availability of large-scale digital computer work was done on surface singularity methods, notably in Germany by Prager and Martensen. [6] In time, more advanced three-dimensional panel codes were developed at Boeing (PANAIR, A502), Lockheed (Quadpan), Douglas (HESS), McDonnell Aircraft (MACAERO), NASA (PMARC) and Analytical Methods (WBAERO, USAERO and VSAERO). Some (PANAIR, HESS and MACAERO) were higher order codes, using higher order distributions of surface singularities, while others (Quadpan, PMARC, USAERO and VSAERO) used single singularities on each surface panel. The advantage of the lower order codes was that they ran much faster on the computers of the time. Today, VSAERO has grown to be a multi-order code and is the most widely used program of this class. It has been used in the development of many submarines, surface ships, automobiles, helicopters, aircrafts, and more recently wind turbines. Its sister code, USAERO is an unsteady panel method that has also been used for modelling such things as high speed trains and racing yachts. The NASA PMARC code from an early version of VSAERO and a derivative of PMARC, named CMARC, is also commercially available. [8]

Over time, panel codes were replaced with higher order panel methods and subsequently CFD (Computational Fluid Dynamics). However, panel codes are still used for preliminary aerodynamic analysis as the time required for an analysis run is significantly less due to a decreased number of elements. [7]

In the two-dimensional realm, a number of Panel Codes have been developed for airfoil analysis and design. The codes typically have a boundary layer analysis included, so that viscous effects can be modelled. Professor Richard Eppler of the University of Stuttgart developed the PROFILE code, partly with NASA funding, which became available in the early 1980's. This was soon followed by MIT Professor Mark Drela's XFOIL code. Both PROFILE and XFOIL incorporate two-dimensional panel codes, with coupled boundary layer codes for airfoil analysis work. [8]

List of some two-dimensional panel codes:

- XFOIL (Open source, recently the most widely used panel code)
- JavaFoil (Open source)
- PROFILE (Prof. Eppler's Program – commercial version)
- PANDA (A Program for Analysis and Design Airfoils – commercial version)
- PABLO (Potential flow around Airfoils with Boundary Layer coupled One-way)
- XFLR5 (Derivate of XFOIL, based on the same algorithm, open source)

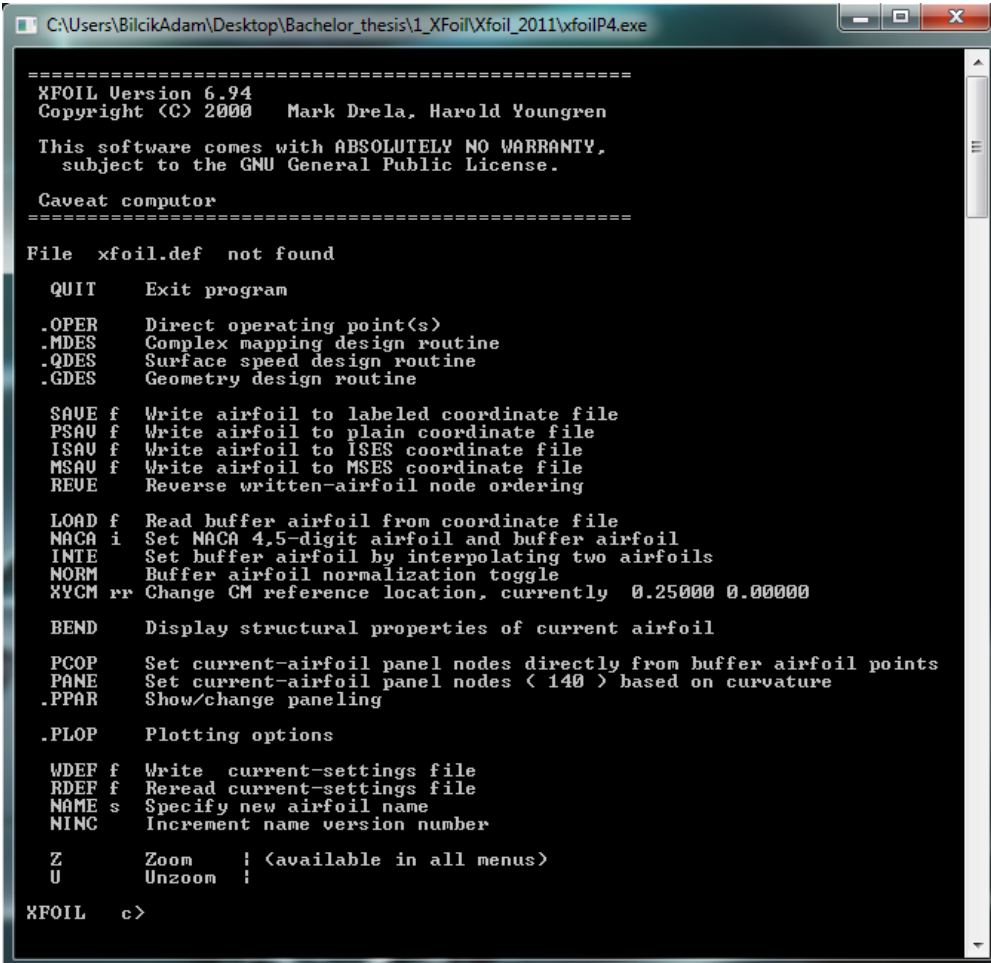
In this study three different panel codes were compared which are publicly released and could be run on the internet or could be downloaded to the computer for free. XFOIL as one of the most widely used panel code, XFLR5 which is re-written XFOIL program to the C/C++ language based on the same algorithms, which was interesting to investigate if the results are the same or not. JavaFoil is another free software which could be used online or downloaded to the computer.

2.2 XFOIL v6.94

XFOIL is a program for the design and analysis of subsonic isolated airfoils. It consists of a collection of menu-driven routines which perform various useful functions. XFOIL 1.0 was written by Mark Drela, Professor of Aerospace Engineering at MIT, in 1986. Since that time program had numerous revisions and upgrades. The source code of XFOIL is Fortran 77 and the program is released under GNU General Public License. [3] Version 6.94 used in this thesis was released on 18th of December 2001.

2.2.1 User's Interface

After the start of the program, the initial window appears. It contains top level menu with a list of commands with short description. Initial window is showed in Figure 2.2.



```

=====
XFOIL Version 6.94
Copyright (C) 2000 Mark Drela, Harold Youngren

This software comes with ABSOLUTELY NO WARRANTY,
subject to the GNU General Public License.

Caveat computer
=====
File xfoil.def not found

QUIT Exit program

.OPER Direct operating point(s)
.MDES Complex mapping design routine
.QDES Surface speed design routine
.GDES Geometry design routine

SAVE f Write airfoil to labeled coordinate file
PSAU f Write airfoil to plain coordinate file
ISAU f Write airfoil to ISES coordinate file
MSAU f Write airfoil to MSES coordinate file
REVE Reverse written-airfoil node ordering

LOAD f Read buffer airfoil from coordinate file
NACA i Set NACA 4,5-digit airfoil and buffer airfoil
INTE Set buffer airfoil by interpolating two airfoils
NORM Buffer airfoil normalization toggle
XYCM rr Change CM reference location, currently 0.25000 0.00000

BEND Display structural properties of current airfoil

PCOP Set current-airfoil panel nodes directly from buffer airfoil points
PANE Set current-airfoil panel nodes ( 140 ) based on curvature
.PPAR Show/change paneling

.PLOP Plotting options

WDEF f Write current-settings file
RDEF f Reread current-settings file
NAME s Specify new airfoil name
NINC Increment name version number

Z Zoom | <available in all menus>
U Unzoom |

XFOIL c>

```

Fig. 2.2. XFOIL initial window

Command "?" displays a list of applicable commands in the given menu or sub-menu. Pushing a key "enter" caused return from sub-menu to the higher menu in tree structure of the program and command "quit" ends the XFOIL.

The first step is to choose calculated airfoil with a command "NACA" and then enter the 4- or 5-digit airfoil designation.

Xfoil also allows import airfoil coordinates from a file. Coordinates in a file must go from trailing edge along the upper surface to the leading edge and back to trailing edge along the lower surface. Zero coordinate must be used only once.

In the next step with a command "**ppar**" a new window is opened called panelling parameters which shows current airfoil with some of the parameters. This window is showed in Figure 2.3. These parameters (number of panel nodes, etc.) can be changed according to the user requests in this sub-menu.

Back in top menu with a command "**oper**" (routine for direct calculation) is opened another sub-menu where input data are set to the program. There are commands which prescribe the parameters of the calculation: activation of viscous mode, input values such as Reynolds number, initial and final angle of attack, increment of angle of attack during the calculation, here is set file name for the results which are showed in Figure 2.4.

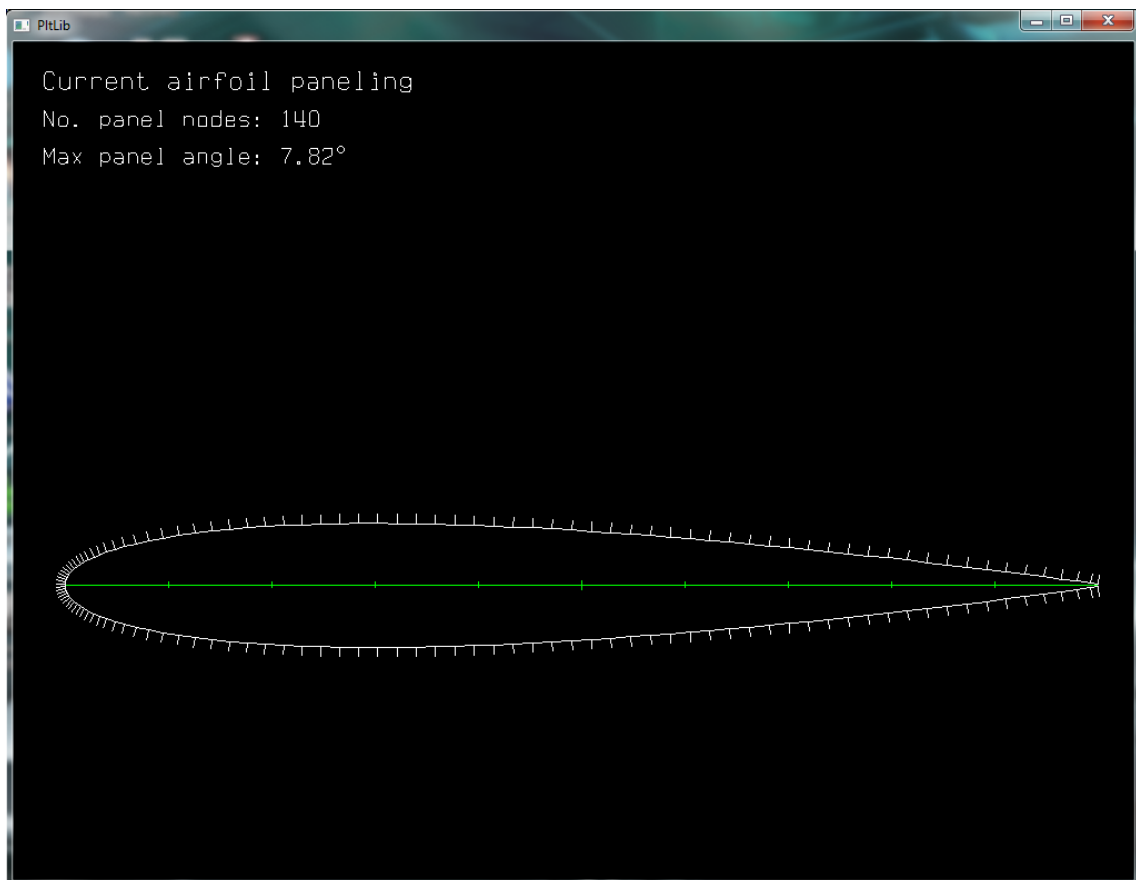


Fig. 2.3. XFOIL panelling parameters window

NACA0012 - Poznámkový blok

Súbor Úpravy Formát Zobrazit' Pomocník

XFOIL Version 6.94

Calculated polar for: NACA 0012

1 1 Reynolds number fixed Mach number fixed

xtrf = 1.000 (top) 1.000 (bottom)
Mach = 0.000 Re = 0.300 e 6 Ncrit = 9.000

alpha	CL	CD	CDp	CM	Top_Xtr	Bot_Xtr
-14.750	-1.0973	0.06530	0.06082	-0.0328	1.0000	0.0281
-14.500	-1.1133	0.06004	0.05538	-0.0352	1.0000	0.0282
-14.250	-1.1248	0.05569	0.05086	-0.0366	1.0000	0.0284
-14.000	-1.1325	0.05205	0.04708	-0.0373	1.0000	0.0286
-13.750	-1.1378	0.04893	0.04383	-0.0374	1.0000	0.0289
-13.500	-1.1414	0.04620	0.04095	-0.0371	1.0000	0.0292
-13.250	-1.1439	0.04376	0.03835	-0.0362	1.0000	0.0296
-13.000	-1.1452	0.04154	0.03598	-0.0349	1.0000	0.0300
-12.750	-1.1441	0.03957	0.03385	-0.0333	1.0000	0.0305
-12.500	-1.1422	0.03771	0.03183	-0.0313	1.0000	0.0311
-12.250	-1.1390	0.03599	0.02993	-0.0290	1.0000	0.0317
-12.000	-1.1340	0.03449	0.02823	-0.0266	1.0000	0.0324
-11.750	-1.1252	0.03326	0.02678	-0.0246	1.0000	0.0331
-11.500	-1.1148	0.03104	0.02439	-0.0230	1.0000	0.0341
-11.250	-1.0998	0.02968	0.02302	-0.0218	1.0000	0.0351
-11.000	-1.0839	0.02865	0.02195	-0.0205	1.0000	0.0362
-10.750	-1.0674	0.02758	0.02078	-0.0192	1.0000	0.0373
-10.500	-1.0501	0.02653	0.01960	-0.0179	1.0000	0.0386
-10.250	-1.0319	0.02562	0.01854	-0.0166	1.0000	0.0397
-10.000	-1.0155	0.02405	0.01689	-0.0152	1.0000	0.0414
-9.750	-0.9971	0.02316	0.01602	-0.0141	1.0000	0.0431
-9.500	-0.9776	0.02245	0.01526	-0.0130	1.0000	0.0451
-9.250	-0.9576	0.02174	0.01445	-0.0118	1.0000	0.0471
-9.000	-0.9392	0.02069	0.01332	-0.0104	1.0000	0.0491
-8.750	-0.9214	0.01976	0.01242	-0.0090	1.0000	0.0516
-8.500	-0.9011	0.01918	0.01182	-0.0078	1.0000	0.0545
-8.250	-0.8798	0.01873	0.01127	-0.0066	1.0000	0.0574
-8.000	-0.8639	0.01767	0.01027	-0.0048	1.0000	0.0613
-7.750	-0.8440	0.01714	0.00972	-0.0034	1.0000	0.0653
-7.500	-0.8244	0.01657	0.00910	-0.0019	1.0000	0.0697
-7.250	-0.8060	0.01592	0.00850	-0.0003	1.0000	0.0757
-7.000	-0.7856	0.01548	0.00801	0.0010	1.0000	0.0817
-6.750	-0.7671	0.01484	0.00744	0.0026	1.0000	0.0902
-6.500	-0.7476	0.01432	0.00695	0.0041	1.0000	0.1000
-6.250	-0.7275	0.01387	0.00653	0.0055	1.0000	0.1120
-6.000	-0.7077	0.01340	0.00613	0.0069	1.0000	0.1272

Fig. 2.4. XFOIL output data file with results

2.3 JavaFoil v2.21

JavaFoil is another computational program for the analysis of airfoils in subsonic flow. It was written by Dr. Martin Hepperle, graduate of University of Stuttgart, as CalcFoil using the "C" language and later on rewritten to "Java" language under the present name JavaFoil. Program is free software which can be used in web browsers or downloaded to your computer and it works with appropriate Java applet.

Version 2.21 used in this thesis was released on 1st March 2014.

The main purpose of JavaFoil is to determine the lift, drag and moment characteristics of airfoils. The program will first calculate the distribution of the velocity on the surface of the airfoil. For this purpose it uses a potential flow analysis module which is based on a higher order panel method (linear varying vorticity distribution). This local velocity and the local pressure are related by the Bernoulli equation. In order to find the lift and the pitching moment coefficient the distribution of the pressure can be integrated along the surface.

Next JavaFoil will calculate the behaviour of the flow layer close to the airfoil surface (the boundary layer). The boundary layer analysis module (a so called integral method) steps along the upper and the lower surfaces of the airfoil, starting at the stagnation point. It solves a set of differential equations to find the various boundary layer parameters. The boundary layer data is then used to calculate the drag of the airfoil from its properties at the trailing edge. Both analysis steps are repeated for each angle of attack, which yields a complete polar of the airfoil for one fixed Reynolds number. [4]

The program also has some limitations, for example it's not possible to analyse airfoils in supersonic flow. JavaFoil analyses airfoils in incompressible flow, which means Mach numbers below $M = 0.25$.

2.3.1 User's Interface

The user interface of the program is divided into several cards where each card contains interface elements for a specific task:

In this thesis is described the Options card as first one, because it has impact to all other cards. There is necessary to set conditions for the computation such as Mach number, air density or speed of sound.

The Geometry card is used to determine the geometry of the airfoil which is calculated. This card shows a list of x- and y-coordinates and plots an airfoil shape. The look of this card is showed in Figure 2.5. JavaFoil allows export or import airfoil geometry in several file types, for example *.txt. Also is possible to import scanned image of an airfoil.

The Modify card can perform various modifications to the airfoil geometry.

The Velocity card shows velocity distribution around airfoil by setting initial angle of attack, final angle of attack and step.

The Flowfield card visualizes the flow around the airfoil in various ways. Push of the button "**Analyze it!**" performs an analysis of an airfoil for the given angle of attack.

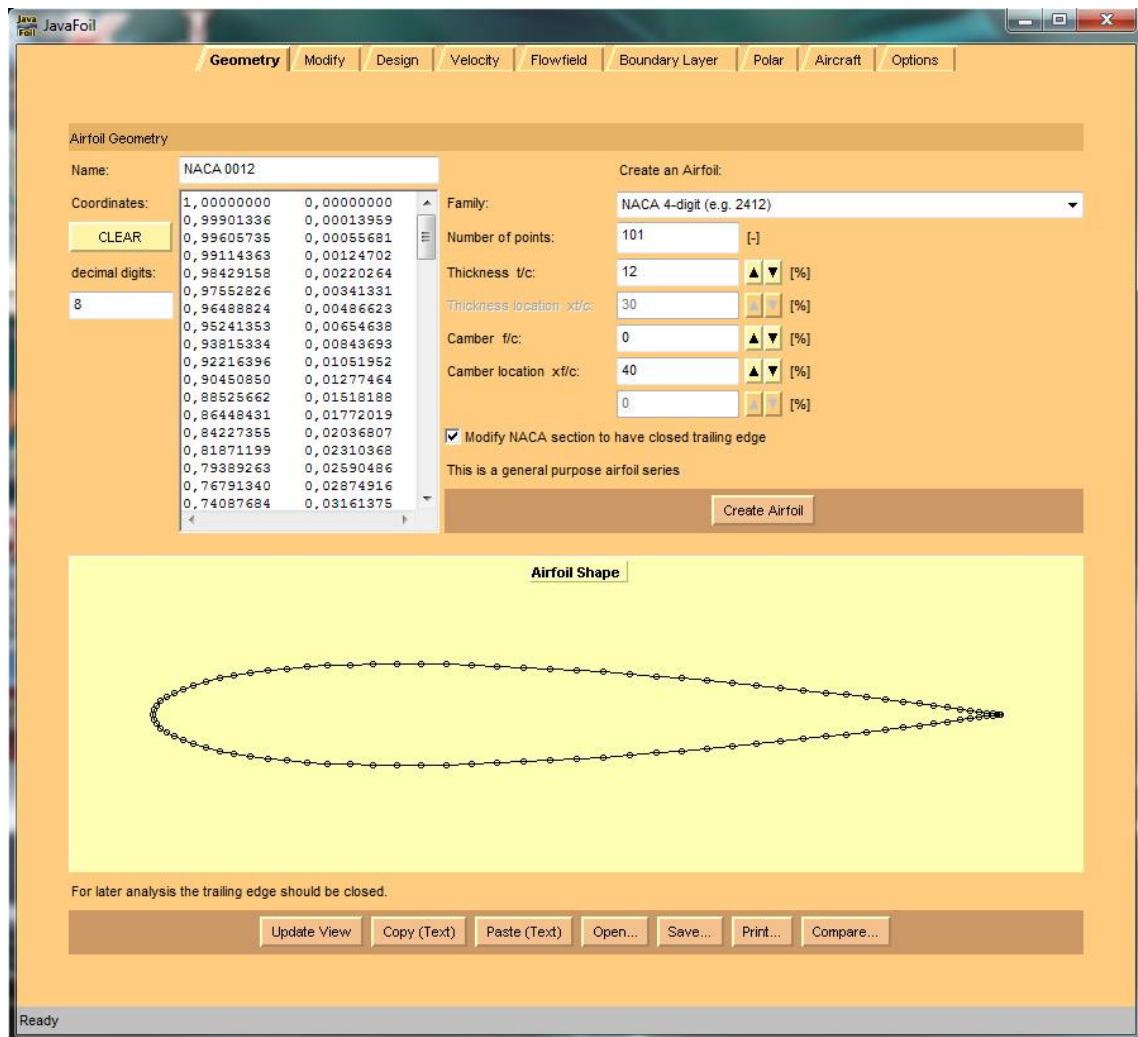


Fig. 2.5. JavaFoil Geometry card

The Polar card shows aerodynamic polar curve. On this card at the bottom is optional to change parameters "Stall model" and "Transition model" which predicts when transition from laminar to turbulent flow occurs. This card is shown in Figure 2.6.

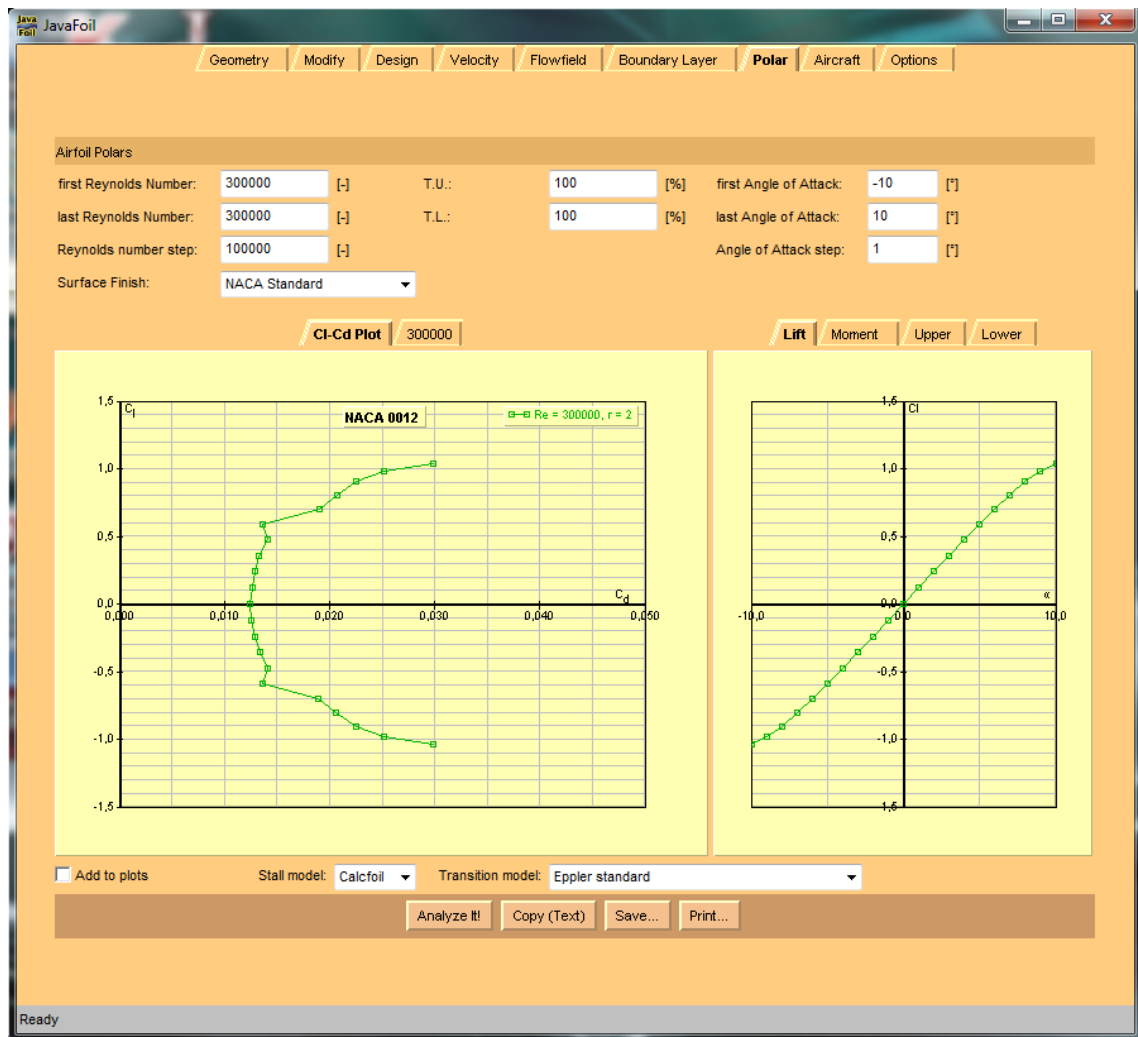


Fig. 2.6. JavaFoil Polar card

Data from JavaFoil could be easily exported to the program such as Microsoft Excel by a button on the down side of the window with the name "**Copy (Text)**". Also there is option to print the results.

2.4 XFLR5 v4.17

Another compared panel code in this thesis was program XFLR5. The algorithms for foil analysis implemented in XFLR5 are exactly the same as those of the original XFOIL code. The program was translated from the original Fortran source code to the C/C++ language and other main goal of creating this program was to provide a more user's friendly interface. Like the original XFOIL, this project has been developed and released in accordance with the principles of the GPL (General Public License).

Wing analysis capabilities have been added in version v2.00. The latest version v4.00 introduced a 3D panel method for wings and planes, including modelling options for fuselages. [5]

2.4.1 User's Interface

The program contains four different "applications". In this part is described an application which is called "**The foil direct analysis routines**" which was used in this thesis for calculation of aerodynamic characteristics of an airfoil NACA 0012 at $Re = 3e5$ for various angles of attack.

After the start of the program and application for foil direct analysis is necessary to load calculated airfoil. XFLR5 is able to load any airfoils from a data file which contains airfoil coordinates or in the main menu by click on "**Designs**" and "**Naca foils**" it could be set NACA 4- or 5-digit airfoil. There is need to set number of panels alongside airfoil surface.

The calculation of aerodynamic characteristics follows by click on "**Polars**" and "**Run Batch Analysis**". There is necessary to enter variables for the computation: first and last Reynolds number with increment, first and last angle of attack with increment, Mach number, etc. Batch Analysis window is showed in Figure 2.7.

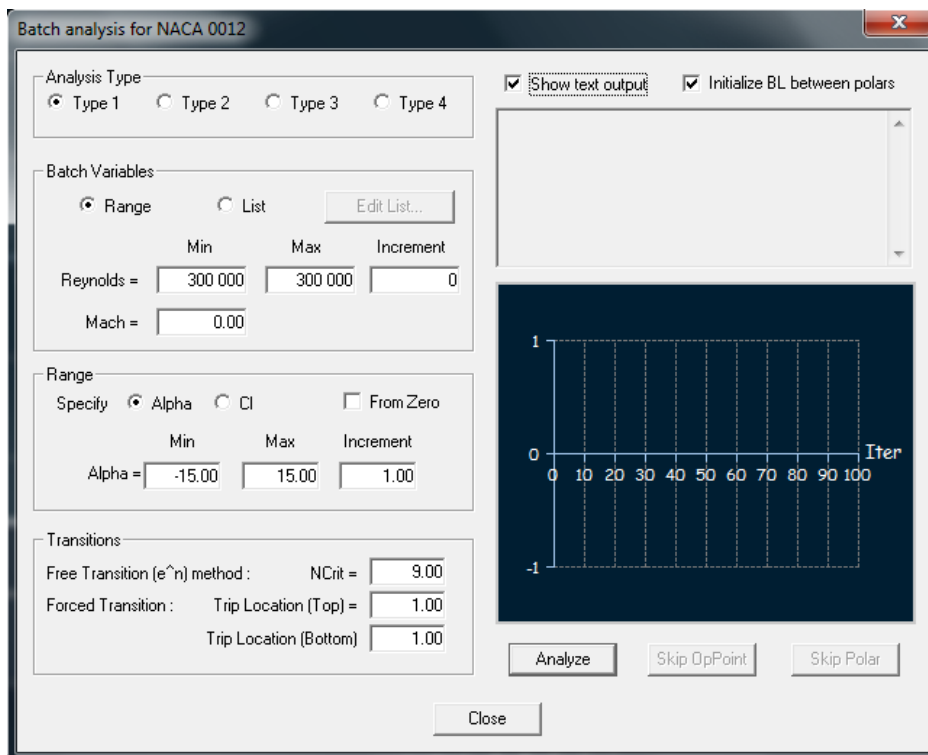


Fig. 2.7. XFLR5 Batch Analysis window

When all the data are set by click on button "Analyze" the computation starts.

Figure 2.8 shows pressure distribution alongside the airfoil surface for various angles of attack with values of c_l , c_d and c_m at the given angle of attack α .

Figure 2.9 shows lift curve, pitching moment curve and polar curve.

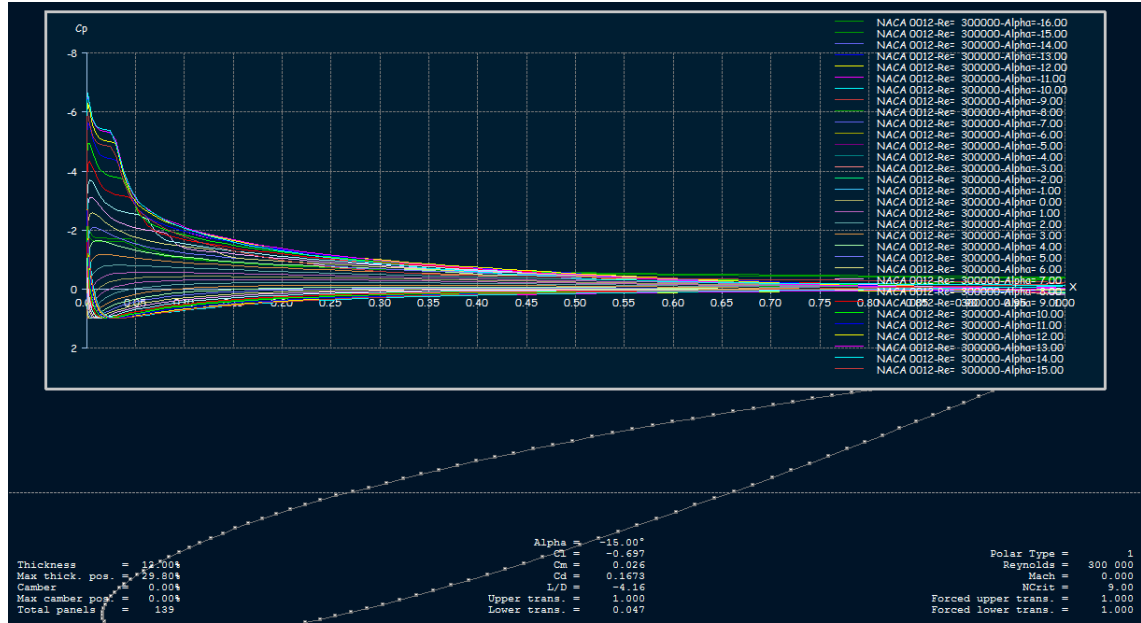


Fig. 2.8. XFLR5 Pressure distribution alongside the airfoil surface

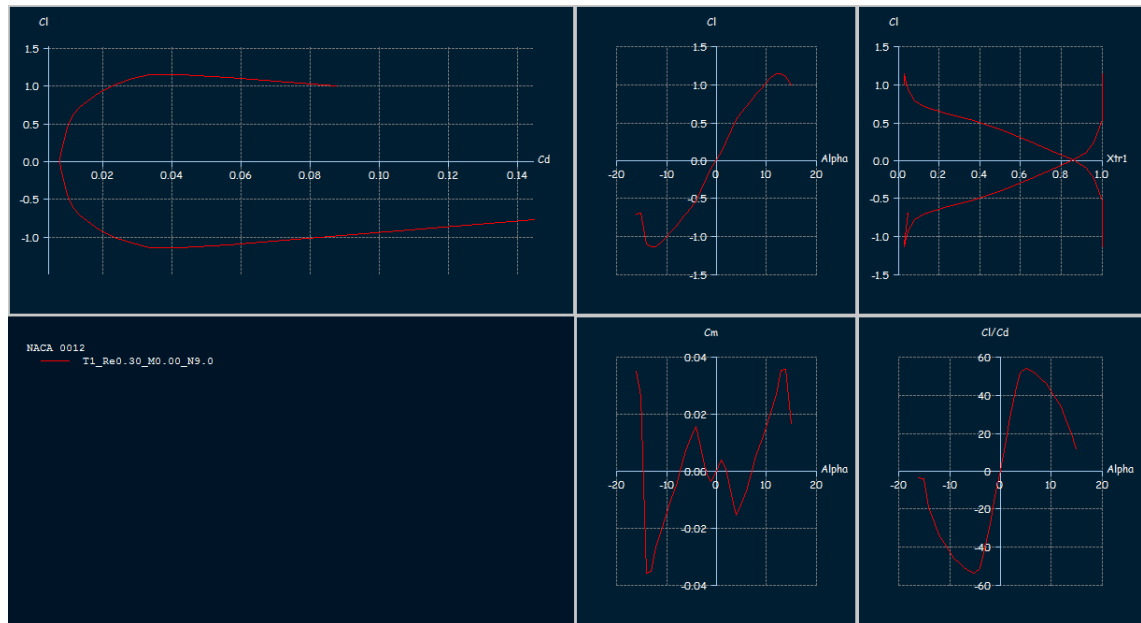


Fig. 2.9. XFLR5 lift curve, pitching moment curve and polar curve visualisation

3 WIND TUNNEL MEASUREMENT

At the very beginning of this thesis it was decided to add wind tunnel measurement and confront its results directly with numerical panel codes. Especially to compare accuracy of the results and effectiveness of the measurement in terms of time required for the measurement and requirements for hardware.

Another objective of this measurement is to become familiarized with the process of determining aerodynamic characteristics of an airfoil from data generated by wind tunnel.

3.1 The Wind Tunnel

A PLINT TE49 is low-speed wind tunnel of Eiffel type with closed measure section in open circuit. The dimensions of the working section are 0.6 x 0.1 x 0.3 meters and the maximum velocity of the air is around 40 m/s ($M = 0.1$). Tunnel constant is approximately 1.059 at $Re = 3e5$. Wind tunnel is shown in Figure 3.1. For the running of the wind tunnel there are used three different programs with different purposes:

1. Program for start and stop of the wind tunnel
2. Remote control of compressor, measuring pressure and wake
3. Data logger which puts results in a text file

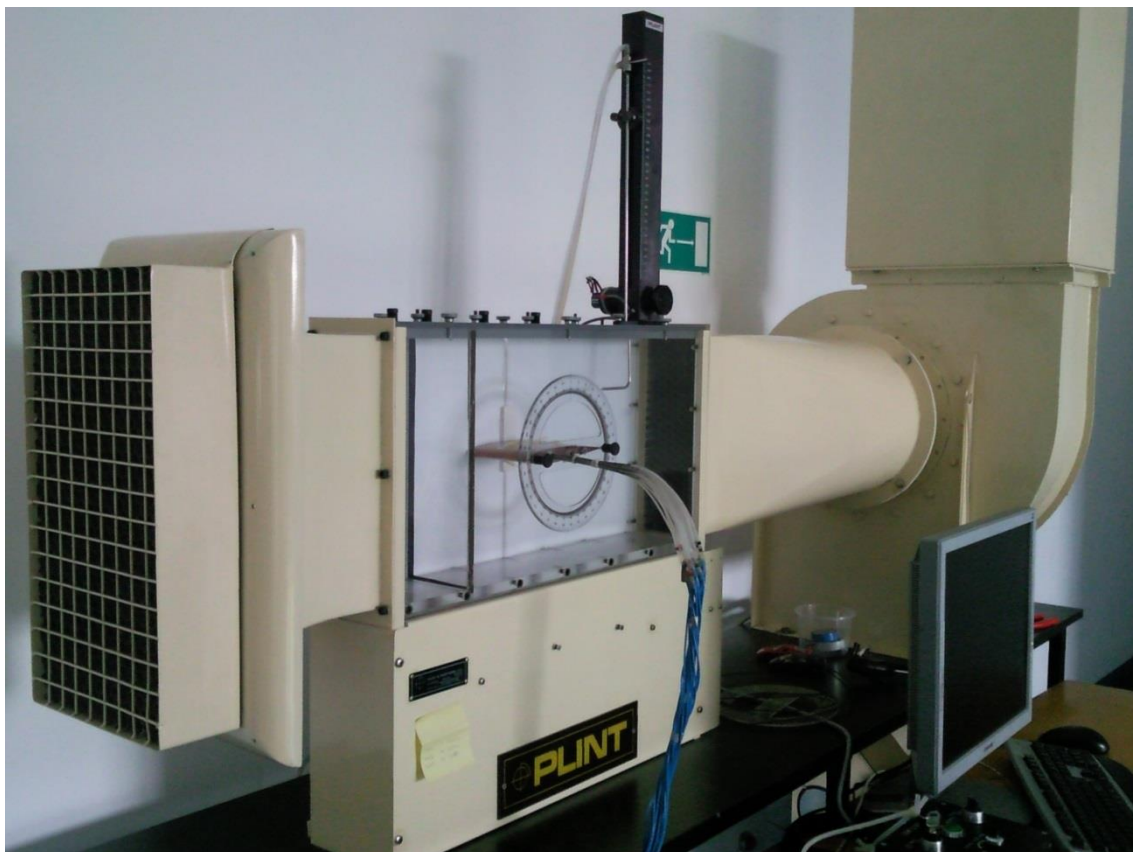


Fig. 3.1. The wind tunnel at the Institute of Aerospace Engineering, Brno University of Technology

3.2 Test Set Up

During this measurement it was used NACA 0012 (chord length = 150.6 mm) airfoil for various angles of attack as in the whole thesis for relevant comparison of results with panel codes. The airfoil is symmetrical which means the aerodynamic characteristics are the same for the both side of the profile. In this wind tunnel the airfoil contains 23 static ports asymmetrically distributed alongside its surface (12 on the lower surface and 11 on the upper surface) and their positions are noted in Figure 3.2. Behind the airfoil in a distance of 60 mm is situated Pitot-static probe for measuring wake. It can traverse its position across the test section. Scheme of the whole test section is in Figure 3.3.

Lower Surface												
Port No.	1	2	3	4	5	6	7	8	9	10	11	12
Distance from LE [mm]	0,8	4,1	10,9	18,6	29,9	44,9	59,9	74,9	89,8	104,8	119,8	135,3
Upper Surface												
Port No.	17	18	19	20	21	22	23	24	25	26	27	
Distance from LE [mm]	2	7,7	15,4	23,3	38,3	53,6	68,4	83,1	98,3	113,7	129,3	

Fig. 3.2. Position of static ports alongside the surface of an airfoil

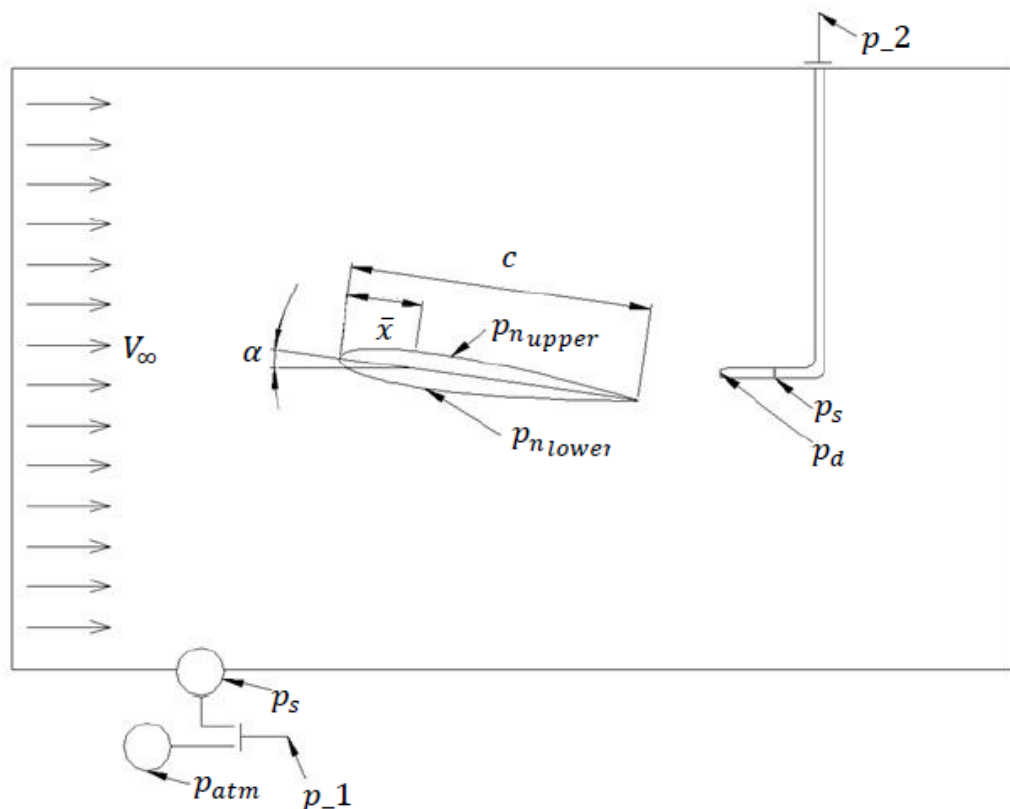


Fig. 3.3. Scheme of wind tunnel test section

3.3 The Measurement

The measurement started at $\alpha = -3^\circ$ due to better mapping of horizontal position of the airfoil. It's continued with an increment of 1 degree. It was needed to find the angle with maximal lift coefficient which is called α_{stall} . The last angle of attack in this measurement was $\alpha = 16^\circ$ which is safely more than α_{stall} .

Reynolds number was approximately similar during the whole measurement and it was approximately $Re = 3e5$. Temperature slightly increased due to work of engine fan.

The measurement of wake started at the position approximately 20 cm over the airfoil and was going down across the test section. There was necessary to have as small steps as possible behind the airfoil for better mapping of the wake. Every step was recorded by pushing a button in a second program.

Measurements conducted within the wind tunnel generate four main sets of data:

- Local static pressure on the lower surface of the airfoil (see Figure 3.4.)
- Local static pressure on the upper surface of the airfoil (see Figure 3.5.)
- Traverse position of the pitot-static probe, dynamic pressure of the free-stream behind and before the airfoil (see Figure 3.6.)
- Air density, air velocity, Reynolds number, barometric pressure

Pressure 1	Pressure 2	Pressure 3	Pressure 4	Pressure 5	Pressure 6	Pressure 7	Pressure 8	Pressure 9	Pressure 10	Pressure 11	Pressure 12
-125,48234	-654,40842	-843,58329	-909,99438	-943,9575	-955,43613	-944,45696	-868,69453	-874,29712	-879,8997	-853,06514	-826,23057
-93,267099	-643,3269	-826,82425	-889,70663	-932,59048	-932,53401	-926,91236	-862,91928	-863,99928	-865,07928	-841,35198	-817,62469
-93,267099	-643,3269	-826,82425	-889,70663	-932,59048	-932,53401	-926,91236	-862,91928	-863,99928	-865,07928	-841,35198	-817,62469
-127,85323	-606,02542	-825,41284	-903,47889	-958,18862	-933,22714	-919,85123	-864,8205	-877,68098	-890,54147	-861,22861	-831,91575
-194,3415	-769,51057	-862,87338	-888,43406	-932,68693	-933,99169	-917,14837	-865,185	-865,40897	-865,63295	-845,32925	-825,02555
-234,41982	-674,83928	-872,54485	-940,7111	-966,21068	-917,94507	-939,70853	-882,12007	-886,58159	-891,04311	-865,36341	-839,68371
-234,41982	-674,83928	-872,54485	-940,7111	-966,21068	-917,94507	-939,70853	-882,12007	-886,58159	-891,04311	-865,36341	-839,68371
-84,929329	-716,81331	-836,71488	-889,9732	-921,10589	-930,32567	-938,81656	-878,61843	-885,37385	-892,12927	-874,81818	-857,50709
-147,88955	-547,28603	-833,28078	-902,08251	-945,46093	-944,90461	-925,02895	-870,43824	-869,93061	-869,42297	-843,3131	-817,20323
-144,47921	-671,89799	-845,17317	-924,19432	-951,81366	-928,71344	-917,92437	-865,50001	-859,41923	-853,33845	-832,51908	-811,69971
-130,43457	-634,44937	-847,91957	-898,61488	-949,41589	-939,9254	-942,70641	-876,38217	-880,79197	-885,20178	-864,66875	-844,13571
-303,89436	-738,08947	-885,6883	-911,88837	-937,4898	-957,87162	-939,8252	-877,5474	-869,15133	-860,75525	-835,47219	-810,18912
-174,08918	-753,29637	-874,62733	-936,74709	-972,08441	-969,93647	-957,81114	-891,61752	-882,00123	-872,38494	-850,35582	-828,32669
-174,08918	-753,29637	-874,62733	-936,74709	-972,08441	-969,93647	-957,81114	-891,61752	-882,00123	-872,38494	-850,35582	-828,32669
-113,8253	-599,00589	-829,45002	-910,98619	-926,47258	-927,30648	-928,10047	-867,88023	-865,5398	-863,19936	-848,53776	-833,87617
-233,7689	-627,79639	-851,04444	-910,88284	-961,37045	-964,08144	-967,62141	-886,89079	-887,81037	-888,72995	-857,71256	-826,69517
-233,7689	-627,79639	-851,04444	-910,88284	-961,37045	-964,08144	-967,62141	-886,89079	-887,81037	-888,72995	-857,71256	-826,69517
-216,28178	-940,67337	-892,01111	-1000,3264	-999,12524	-1001,536	-971,13006	-896,323	-896,81705	-897,3111	-872,17555	-847,04
-90,549403	-588,0022	-818,30654	-902,32649	-941,93064	-932,35118	-922,02072	-879,61246	-865,4426	-851,27275	-838,49805	-825,72335
-90,549403	-588,0022	-818,30654	-902,32649	-941,93064	-932,35118	-922,02072	-879,61246	-865,4426	-851,27275	-838,49805	-825,72335
-80,949312	-560,91405	-818,56029	-894,76187	-930,99101	-939,15945	-925,38619	-869,42447	-863,90425	-858,38402	-840,67636	-822,9687
-125,75258	-558,81793	-824,88874	-896,74735	-948,6663	-951,9634	-942,53818	-879,74153	-875,52813	-871,31472	-851,10786	-830,901
-75,374846	-611,24223	-830,64216	-909,78122	-954,49857	-944,1012	-923,93734	-871,43298	-869,46641	-867,49984	-853,42814	-839,35644
-75,374846	-611,24223	-830,64216	-909,78122	-954,49857	-944,1012	-923,93734	-871,43298	-869,46641	-867,49984	-853,42814	-839,35644
-141,2447	-496,81836	-839,93113	-910,05918	-915,76394	-930,49854	-921,32253	-869,53467	-873,13436	-876,73406	-851,4349	-826,13574
-142,66589	-714,51687	-854,43937	-900,46869	-929,54663	-937,12776	-932,39498	-875,99246	-872,21317	-868,43388	-847,26391	-826,09394
-156,30576	-602,95125	-842,31187	-900,55943	-952,38493	-962,77647	-932,056	-887,51238	-876,05657	-864,60075	-845,26485	-825,92895
-163,55899	-572,01452	-835,91032	-882,80817	-919,94369	-933,07915	-940,73713	-874,75903	-874,3935	-874,02797	-845,95704	-817,88612
-163,55899	-572,01452	-835,91032	-882,80817	-919,94369	-933,07915	-940,73713	-874,75903	-874,3935	-874,02797	-845,95704	-817,88612
-128,91358	-684,71557	-852,69846	-908,51901	-936,85765	-930,10296	-912,1898	-870,08326	-870,54974	-871,01622	-841,26715	-811,51809

Fig. 3.4. Data file with pressures on the lower surface of the airfoil

Pressure 17	Pressure 18	Pressure 19	Pressure 20	Pressure 21	Pressure 22	Pressure 23	Pressure 24	Pressure 25	Pressure 26	Pressure 27
-1652,2578	-1705,0008	-1713,1617	-1456,9779	-1260,3867	-1141,2523	-1160,2363	-1098,8407	-1037,4451	-1002,2893	-889,1305
-1599,8085	-1595,7395	-1588,0533	-1434,8137	-1211,2947	-1142,2885	-1141,4292	-1082,1233	-1022,8174	-967,73288	-865,13175
-1599,8085	-1595,7395	-1588,0533	-1434,8137	-1211,2947	-1142,2885	-1141,4292	-1082,1233	-1022,8174	-967,73288	-865,13175
-1634,6554	-1627,5565	-1655,4138	-1459,2578	-1235,4898	-1167,638	-1149,4594	-1092,8616	-1036,2639	-988,7438	-865,67052
-1675,6937	-1673,7938	-1693,9763	-1431,913	-1227,7232	-1165,43	-1158,2042	-1105,3187	-1052,4331	-1007,8266	-874,62929
-1689,7924	-1652,6634	-1680,4944	-1447,8461	-1232,3953	-1155,9628	-1156,7213	-1112,8758	-1069,0303	-1007,8292	-867,83232
-1689,7924	-1652,6634	-1680,4944	-1447,8461	-1232,3953	-1155,9628	-1156,7213	-1112,8758	-1069,0303	-1007,8292	-867,83232
-1636,3798	-1582,7417	-1612,0973	-1447,3069	-1215,6992	-1126,7393	-1139,8351	-1085,6111	-1031,3872	-1000,9738	-891,14548
-1600,4543	-1694,5797	-1586,3214	-1435,9321	-1243,425	-1166,0716	-1152,862	-1097,5984	-1042,3349	-1004,7906	-868,54817
-1672,4641	-1646,3137	-1623,587	-1461,0957	-1240,7632	-1163,0901	-1139,3883	-1086,1321	-1032,876	-973,42081	-877,35558
-1626,7811	-1588,1014	-1592,4914	-1431,7271	-1257,708	-1151,1335	-1168,9588	-1108,7026	-1048,4465	-986,14851	-874,69893
-1644,7459	-1634,227	-1670,8468	-1445,0471	-1229,2616	-1158,1153	-1140,5656	-1091,7155	-1042,8653	-1008,5895	-882,50787
-1745,5827	-1636,9609	-1611,4298	-1435,5054	-1228,8862	-1162,8703	-1133,604	-1077,3356	-1021,0671	-977,91785	-875,73804
-1745,5827	-1636,9609	-1611,4298	-1435,5054	-1228,8862	-1162,8703	-1133,604	-1077,3356	-1021,0671	-977,91785	-875,73804
-1665,6893	-1557,4696	-1653,1229	-1453,6157	-1250,2832	-1152,4068	-1141,9778	-1082,1027	-1022,2276	-965,43676	-939,99119
-1605,7419	-1618,4017	-1628,201	-1427,2096	-1240,9481	-1152,311	-1142,646	-1091,9995	-1041,3531	-981,83418	-869,25294
-1605,7419	-1618,4017	-1628,201	-1427,2096	-1240,9481	-1152,311	-1142,646	-1091,9995	-1041,3531	-981,83418	-869,25294
-1738,9106	-1771,3361	-1662,8289	-1444,618	-1230,083	-1147,2809	-1112,8795	-1069,4856	-1026,0918	-977,97046	-857,44163
-1643,9518	-1612,059	-1568,9435	-1405,7336	-1234,1855	-1154,3957	-1140,4162	-1082,2786	-1024,141	-977,32159	-873,25205
-1643,9518	-1612,059	-1568,9435	-1405,7336	-1234,1855	-1154,3957	-1140,4162	-1082,2786	-1024,141	-977,32159	-873,25205
-1820,3022	-1716,3014	-1602,2332	-1422,7955	-1244,4588	-1176,4838	-1175,8509	-1113,2844	-1050,718	-1025,6223	-908,75618
-1555,3942	-1671,7896	-1601,7211	-1432,554	-1236,2562	-1160,8852	-1149,6181	-1095,5813	-1041,5444	-963,08663	-880,25406
-1646,195	-1587,4696	-1648,1758	-1464,7793	-1233,4929	-1155,975	-1140,7619	-1091,5064	-1042,251	-977,58425	-868,57207
-1646,195	-1587,4696	-1648,1758	-1464,7793	-1233,4929	-1155,975	-1140,7619	-1091,5064	-1042,251	-977,58425	-868,57207
-1728,5429	-1645,7071	-1670,9474	-1459,9783	-1238,0422	-1153,6439	-1152,1412	-1084,4543	-1016,7674	-983,34358	-881,20957
-1723,9848	-1649,1443	-1659,1278	-1438,1695	-1225,5894	-1154,2406	-1130,1284	-1075,5971	-1021,0657	-992,30686	-880,73773
-1703,9888	-1671,4445	-1629,7883	-1435,5124	-1227,1766	-1135,3457	-1121,8042	-1072,0005	-1022,1969	-977,67492	-900,07742
-1617,8304	-1655,8571	-1596,1622	-1424,8087	-1220,5625	-1131,1803	-1138,3937	-1092,2923	-1046,1909	-971,96196	-892,768
-1617,8304	-1655,8571	-1596,1622	-1424,8087	-1220,5625	-1131,1803	-1138,3937	-1092,2923	-1046,1909	-971,96196	-892,768
-1698,6539	-1647,4912	-1672,9154	-1463,2458	-1219,3686	-1140,6716	-1127,9526	-1091,946	-1055,9394	-1006,2334	-880,79148

Fig. 3.5. Data file with pressures on the upper surface of the airfoil

Point index	Time	PB temp	Pressure_1	Pressure_2	Bar_pressure	Temperature	Traverse_position
578	1156,406739	16,107664	795,480096	825,053378	980,4265	19,618363	70,481452
580	1160,069564	16,074232	788,957908	826,871812	980,430668	19,617871	68,758856
580	1160,069564	16,074232	788,957908	826,871812	980,430668	19,617871	68,758856
582	1163,550493	16,109263	797,54113	821,132254	980,429402	19,616992	65,019424
583	1165,306703	16,122523	787,802018	817,784574	980,427685	19,622651	63,100038
584	1167,160735	16,122652	785,093068	823,334874	980,429172	19,621378	62,146246
584	1167,160735	16,122652	785,093068	823,334874	980,429172	19,621378	62,146246
585	1169,173012	16,104336	779,372028	823,138199	980,424168	19,618251	61,10345
586	1171,306008	16,12696	782,842876	804,520676	980,424644	19,618376	59,777678
587	1173,233141	16,177392	788,072323	815,134235	980,431065	19,619611	58,402667
588	1175,255862	16,102995	789,798917	804,684227	980,427541	19,618706	57,265764
589	1176,997104	16,133564	792,008775	750,372528	980,413632	19,618293	56,226342
590	1179,06391	16,127244	781,539293	756,385619	980,419706	19,617046	55,173534
590	1179,06391	16,127244	781,539293	756,385619	980,419706	19,617046	55,173534
591	1181,28519	16,154485	786,843081	716,132417	980,411415	19,618553	54,14427
592	1183,505877	16,091361	785,311027	685,081945	980,408977	19,619591	52,66867
592	1183,505877	16,091361	785,311027	685,081945	980,408977	19,619591	52,66867
593	1185,680518	16,079546	785,492516	643,467601	980,394175	19,618982	51,334019
594	1187,832568	16,102866	782,341506	663,797098	980,401113	19,618155	49,980401
594	1187,832568	16,102866	782,341506	663,797098	980,401113	19,618155	49,980401
595	1189,968766	16,088497	776,07561	734,147199	980,41853	19,617447	48,576478
596	1192,181046	16,086047	774,929133	758,517903	980,427799	19,617923	47,133103
597	1194,289845	16,159205	784,18373	795,681236	980,435983	19,617028	46,101972
597	1194,289845	16,159205	784,18373	795,681236	980,435983	19,617028	46,101972
598	1196,582937	16,127321	781,105343	807,85573	980,437155	19,623354	44,8952
599	1198,701486	16,120691	773,812052	806,406926	980,444449	19,628114	43,666624
600	1200,788693	16,099899	777,060176	811,431349	980,442114	19,626838	42,63295
601	1202,827354	16,082255	779,135212	822,598723	980,445158	19,640918	40,950567
601	1202,827354	16,082255	779,135212	822,598723	980,445158	19,640918	40,950567
602	1204,614204	16,123709	772,22475	821,207157	980,445101	19,640351	38,176023

Fig. 3.6. Data file with other wind tunnel generated data

4 NACA REPORT

The National Advisory Committee for Aeronautics (NACA) was a U.S. federal agency founded on 3rd March 1915, to undertake, promote, and institutionalize aeronautical research. NACA after its end on 1st October of 1958 was transformed to the newly created National Aeronautics and Space Administration (NASA). [10]

In 1929, NACA began studying the characteristics of systematic series of airfoils in an effort to find the shapes that were best suited for specific purposes. Families of airfoils constructed according to a certain plan were tested and their characteristics recorded. [1] NACA researchers operated many wind tunnels, engine test stands and flight test facilities.

There is a NACA report No. 586 made in 1935 for various airfoils design. Results from this report for NACA 0012 airfoil for various Reynolds numbers are shown in Figure 4.1 for lift curve and in Figure 4.2 for polar curve.

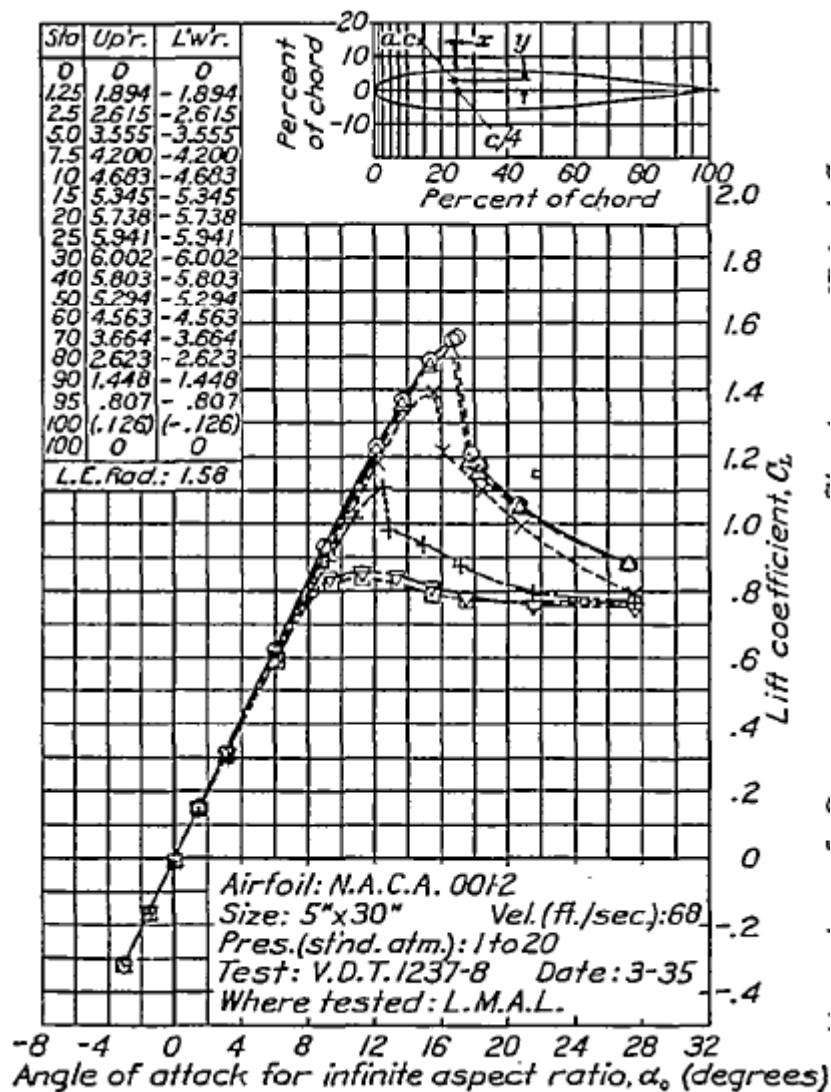


Fig. 4.1. Lift curve for NACA 0012 airfoil for various Reynolds numbers

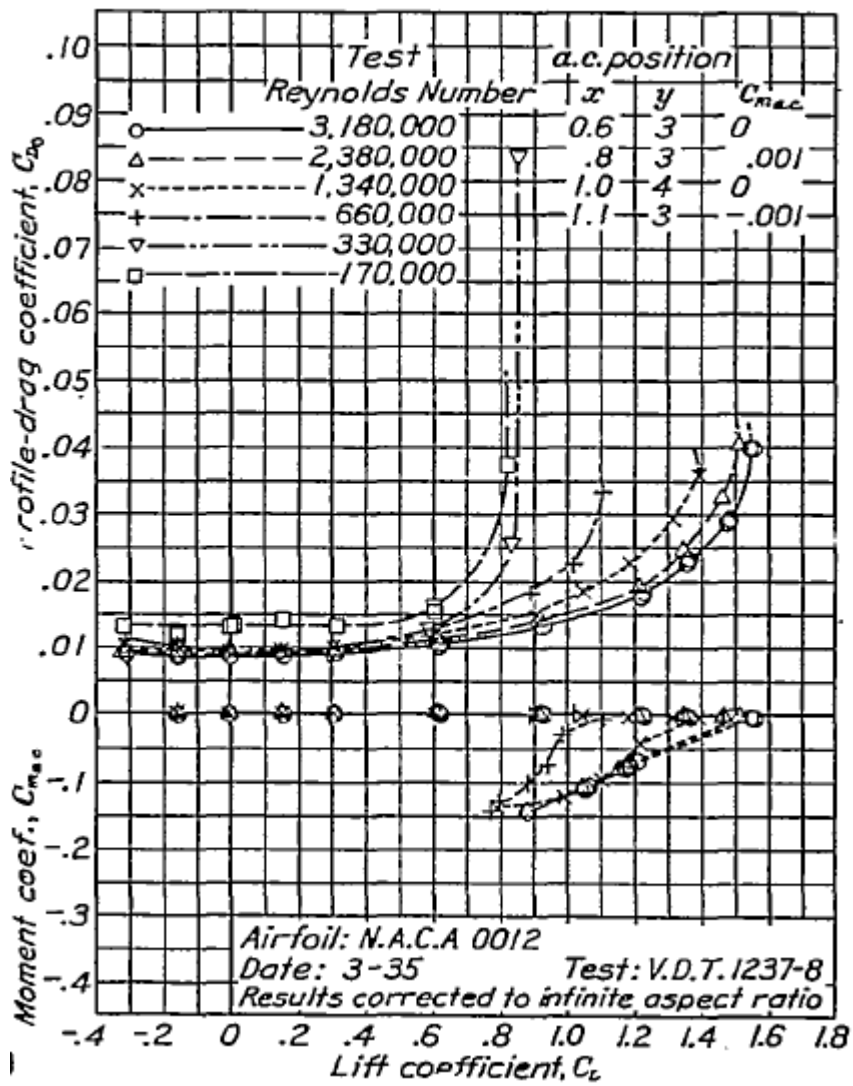


Fig. 4.2. Polar curve for NACA 0012 airfoil for various Reynolds numbers

5 COMAPARISON OF RESULTS

There are recorded results from panel codes: XFOIL, JavaFoil and XFLR5 added by results from wind tunnel and NACA report No. 586.

For all measurements it was used NACA 0012 airfoil which could be considered as a benchmark profile as one of the most tested airfoil and also by the disposition of Brno University of Technology (BUT) wind tunnel. Reynolds number was set to $Re = 300000$ with the primary use in the wind tunnel. All panel codes computed with airfoil divided into 140 panels and at Mach 0.0. Transition criterion was choose $n_{crit} = 9$, which corresponds with average wind tunnel and is the most common choice.

This comparison of results is divided into three parts: lift curve, pitching moment curve and polar curve. The final values of aerodynamic coefficients from panel codes computation were recorded in a table shown on Figure 5.1, data from wind tunnel measurement and data from NACA report were recorded in table shown on Figure 5.2.

13.5.2014	Xfoil 6.94			JavaFoil 2.21			XFLR5 4.17		
Angle of Attack (AOA)	Cl	Cd	Cm _{0,25}	Cl	Cd	Cm _{0,25}	Cl	Cd	Cm _{0,25}
-15	-1,0759	0,07171	-0,0292	-0,999	0,1359	0,008	-0,697	0,1673	0,026
-14	-1,1325	0,05205	-0,0373	-0,999	0,11986	0,008	-1,097	0,0561	-0,036
-13	-1,1452	0,04154	-0,0349	-0,988	0,10477	0,008	-1,136	0,0426	-0,035
-12	-1,134	0,03449	-0,0266	-0,968	0,09016	0,008	-1,135	0,0336	-0,027
-11	-1,0839	0,02865	-0,0205	-0,97	0,06479	0,01	-1,082	0,0286	-0,021
-10	-1,0155	0,02405	-0,0152	-1,034	0,0311	0,011	-1,015	0,0241	-0,015
-9	-0,9392	0,02069	-0,0104	-0,985	0,0263	0,011	-0,94	0,0205	-0,01
-8	-0,8639	0,01767	-0,0048	-0,904	0,02388	0,009	-0,862	0,0178	-0,005
-7	-0,7856	0,01548	0,001	-0,808	0,02202	0,008	-0,785	0,0155	0,001
-6	-0,7077	0,0134	0,0069	-0,703	0,0187	0,007	-0,708	0,0134	0,007
-5	-0,626	0,0117	0,0118	-0,592	0,0186	0,006	-0,626	0,0117	0,012
-4	-0,5384	0,01056	0,0154	-0,477	0,01861	0,005	-0,539	0,0106	0,016
-3	-0,3979	0,00963	0,0084	-0,359	0,01769	0,004	-0,397	0,0096	0,008
-2	-0,2371	0,00874	-0,0017	-0,24	0,0181	0,002	-0,24	0,0088	-0,001
-1	-0,1074	0,008	-0,0037	-0,12	0,0169	0,001	-0,106	0,008	-0,004
0	0	0,00768	0	0	0,01669	0	0	0,0077	0
1	0,1074	0,008	0,0037	0,12	0,01689	-0,001	0,106	0,008	0,004
2	0,2371	0,00874	0,0017	0,24	0,01812	-0,002	0,24	0,0087	0,001
3	0,3979	0,00963	-0,0084	0,359	0,01767	-0,004	0,397	0,0096	-0,008
4	0,5383	0,01056	-0,0154	0,477	0,0186	-0,005	0,539	0,0106	-0,016
5	0,6259	0,0117	-0,0118	0,592	0,01864	-0,006	0,626	0,0117	-0,012
6	0,7076	0,01339	-0,0069	0,703	0,01873	-0,007	0,708	0,0134	-0,007
7	0,7855	0,01547	-0,001	0,808	0,02202	-0,008	0,785	0,0155	-0,001
8	0,8639	0,01767	0,0048	0,904	0,02388	-0,009	0,862	0,0178	0,005
9	0,9393	0,02069	0,0104	0,985	0,0263	-0,011	0,94	0,0205	0,01
10	1,0156	0,02405	0,0152	1,034	0,0311	-0,011	1,015	0,0241	0,015
11	1,0842	0,02865	0,0204	0,97	0,06478	-0,01	1,082	0,0286	0,021
12	1,1345	0,0345	0,0265	0,968	0,09016	-0,008	1,135	0,0336	0,027
13	1,1461	0,04154	0,0348	0,988	0,10477	-0,008	1,187	0,0426	0,035
14	1,134	0,05202	0,0371	0,999	0,11986	-0,008	1,098	0,0562	0,036
15	1,0774	0,07172	0,029	0,999	0,13589	-0,008	0,989	0,0874	0,017

Fig. 5.1. Result from panel codes recorded in Microsoft Excel table

28.5.2014	BUT Wind Tunnel PLINT			NACA Report No. 586 (Re = 3.3e5)		
Angle of Attack (AOA)	Cl	Cd	Cm _{0,25}	Cl	Cd	Cm _{0,25}
-15	-1,13157	0,187275	0,196324			
-14	-1,1051	0,15569	0,175913	-0,83		
-13	-1,10472	0,141078	0,133845	-0,8475		
-12	-1,08516	0,125204	0,110399	-0,875		
-11	-1,04448	0,067975	0,083623	-0,8685		
-10	-1,00941	0,061435	0,068644	-0,84		
-9	-0,95929	0,046335	0,064247	-0,8035		
-8	-0,88905	0,039163	0,066349	-0,76		
-7	-0,78063	0,038324	0,061557	-0,67		
-6	-0,67833	0,03874	0,059741	-0,58		
-5	-0,57316	0,037386	0,054421	-0,49		
-4	-0,45743	0,038697	0,045004	-0,4		
-3	-0,35207	0,035161	0,037293	-0,3		
-2	-0,240864	0,037964	0,015991	-0,2		
-1	-0,144169	0,03565	0,005324	-0,1		
0	0,049622	0,036829	-0,00531	0		
1	0,144169	0,03565	-0,01539	0,1		
2	0,240864	0,037964	-0,02546	0,2		
3	0,352074	0,035161	-0,03729	0,3		
4	0,457429	0,038697	-0,045	0,4		
5	0,573156	0,037386	-0,05442	0,49		
6	0,678328	0,03874	-0,05974	0,58		
7	0,780625	0,038324	-0,06156	0,67		
8	0,889049	0,039163	-0,06635	0,76		
9	0,959294	0,046335	-0,06425	0,8035		
10	1,009411	0,061435	-0,06864	0,84		
11	1,044477	0,067975	-0,08362	0,8685		
12	1,085159	0,125204	-0,1104	0,875		
13	1,104718	0,141078	-0,13385	0,8475		
14	1,105098	0,15569	-0,17591	0,83		
15	1,131575	0,187275	-0,19632			

Fig. 5.2. Result from wind tunnel and NACA report recorded in Microsoft Excel table

NACA Report No. 586 was performed at various Reynolds numbers. To this thesis was chosen the closest value to the panel codes computation and wind tunnel measurement which was $Re = 330\ 000$. There are missing coefficients for drag and pitching moment which was caused by a difficulty to read data from a graph.

5.1 Lift curve

Lift curve displays lift coefficient c_l versus angle of attack α . The lift coefficient varies linearly with the geometric angle of attack, and the slope of the lift curve m_0 is almost 2π . Lift curve of panel codes and wind tunnel has almost the same steep slope of the lift curve, only NACA report has not that steep slope of the lift curve. Results of XFOIL and XFLR5 can be compared as the same. They both reached α_{stall} at $\alpha = 13^\circ$. JavaFoil reached α_{stall} at $\alpha = 9^\circ$, NACA report at $\alpha = 12^\circ$. During measurement in the wind tunnel it wasn't reached α_{stall} . Lift curve is shown on Figure 5.3.

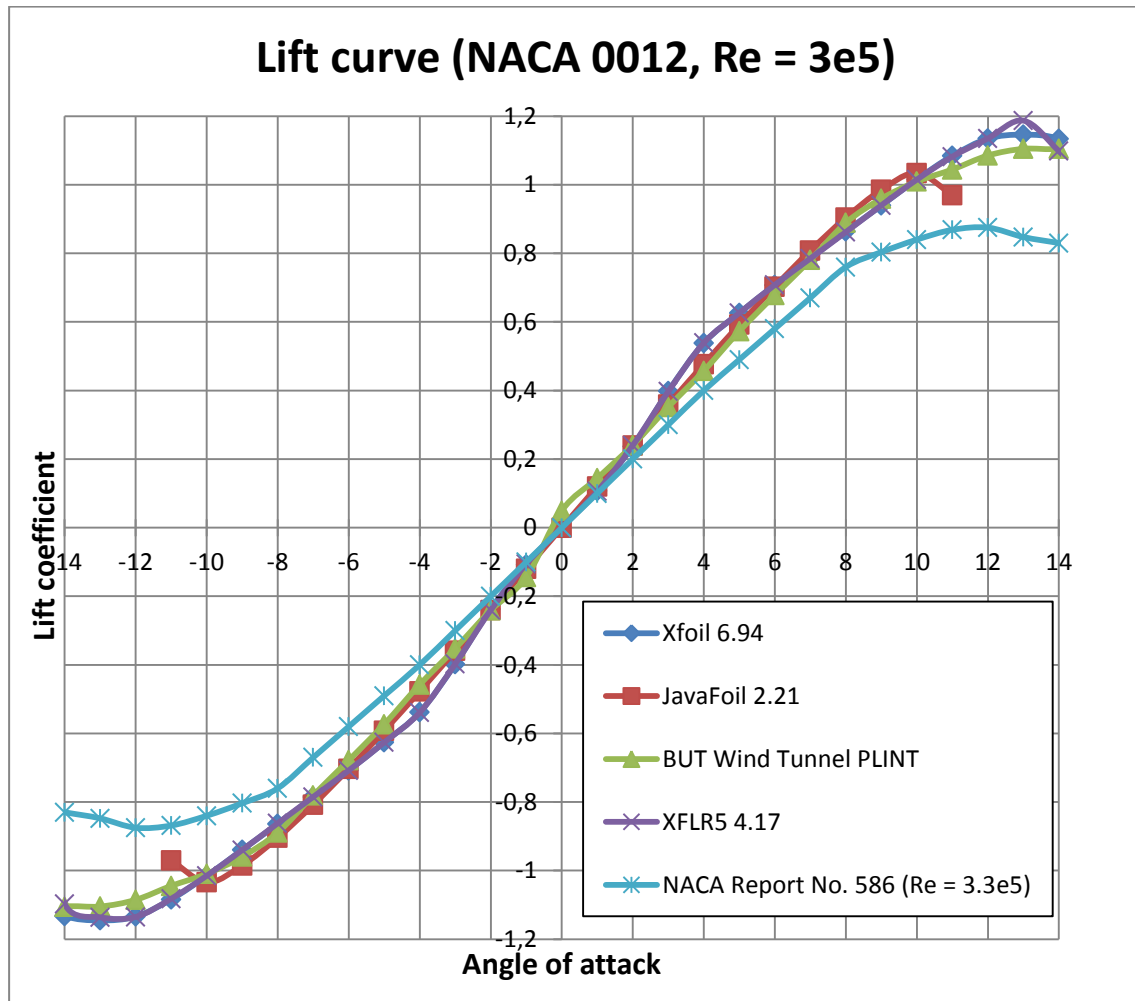


Fig. 5.3. Lift curve of NACA 0012 airfoil. $Re = 3 \times 10^5$

The highest lift coefficient c_{lmax} was reached by XFOIL/XFLR5 code and on the other side is NACA report with the lift coefficient c_{lmax} approaching the value $c_{lmax} = 0.9$.

All curves in the graph are going through the zero lift coefficient at zero angle of attack α , with respect to the chapter 1.1.

5.2 Pitching moment curve

Pitching moment curve displays $c_{m0,25}$ versus angle of attack α . Same as in previous lift curve, XFOIL and XFLR5 has the same results with non-linear slope of the pitching moment curve around the beginning of the coordinate system. Pitching moment curve calculated by JavaFoil can be compared as linear. Curve generated by the wind tunnel is also linear but it has the steepest slope of the curve. Pitching moment curve is shown on Figure 5.4.

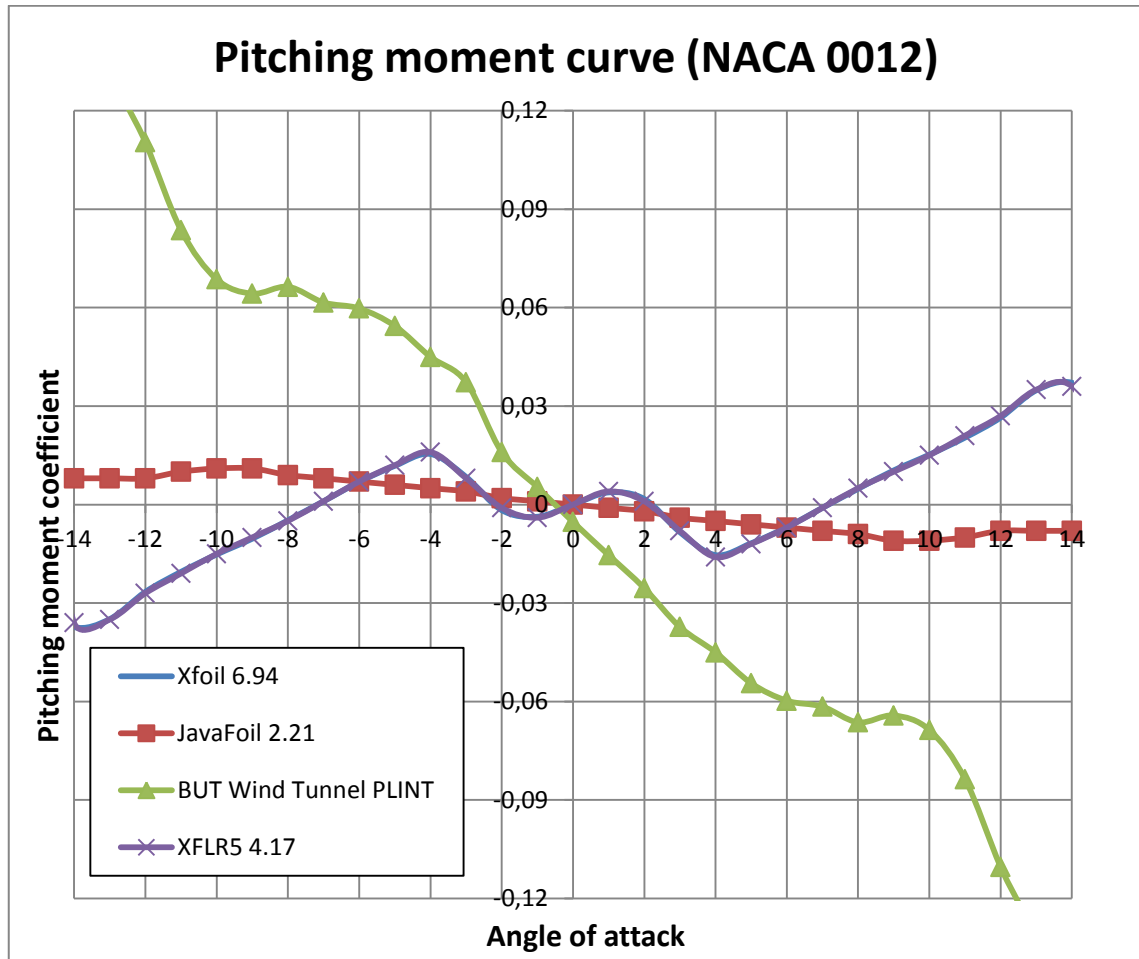


Fig. 5.4. Pitching moment curve of NACA 0012 airfoil. $Re = 3 \times 10^5$

5.3 Polar curve

Polar curve displays lift coefficient c_l versus drag coefficient c_d . Results of XFOIL and XFLR5 are almost the same. Results are slightly different at higher angles of attack where drag coefficient is different. Result from JavaFoil had the values of drag between XFOIL/XFLR5 and wind tunnel. On the other side wind tunnel measurement reached the highest values of drag at low angles of attack. Polar curve is shown on Figure 5.5. Figure 5.6 displays polar curves in comparison between panel codes, wind tunnel measurement and NACA report No. 586.

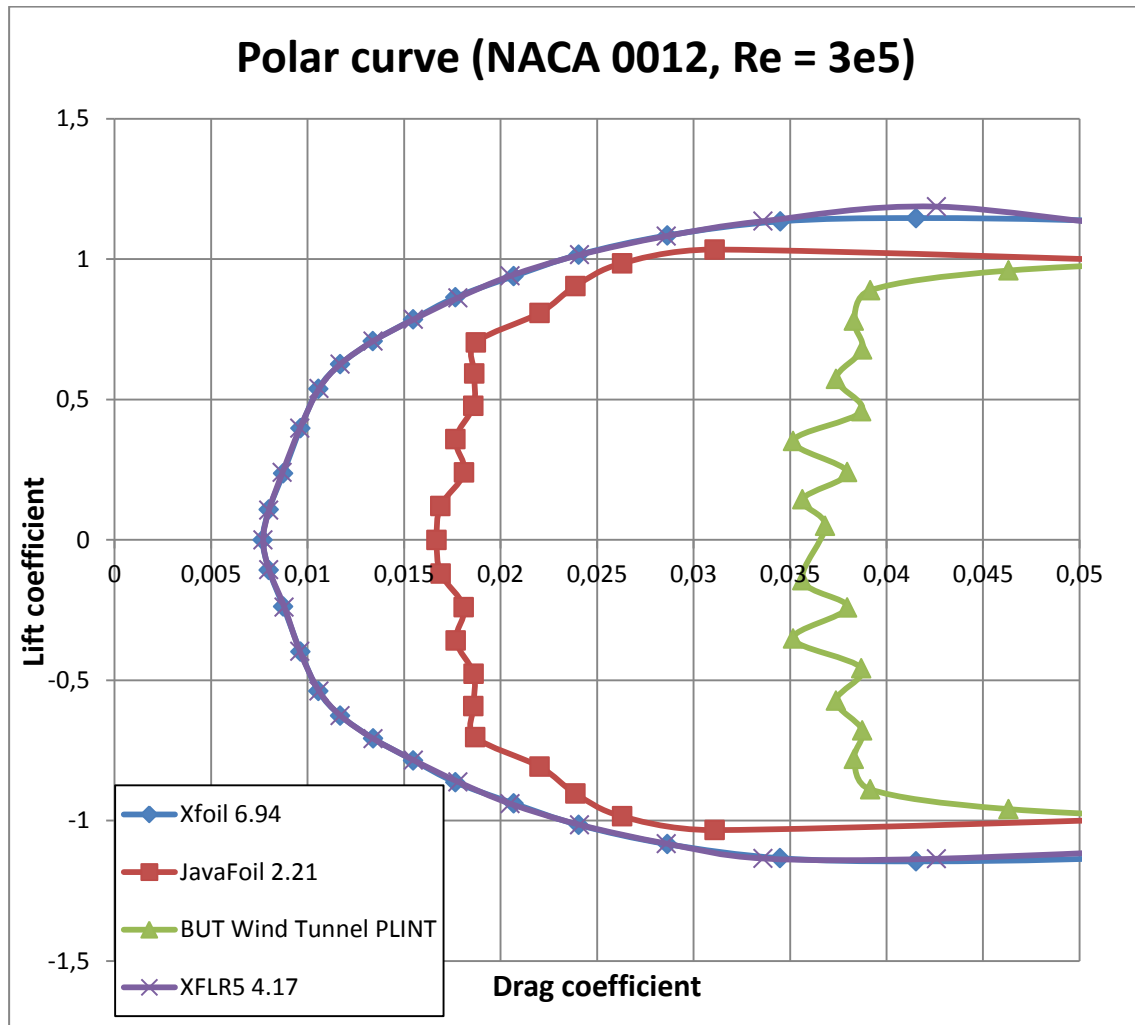


Fig. 5.5. Polar curve of NACA 0012 airfoil. $Re = 3 \times 10^5$

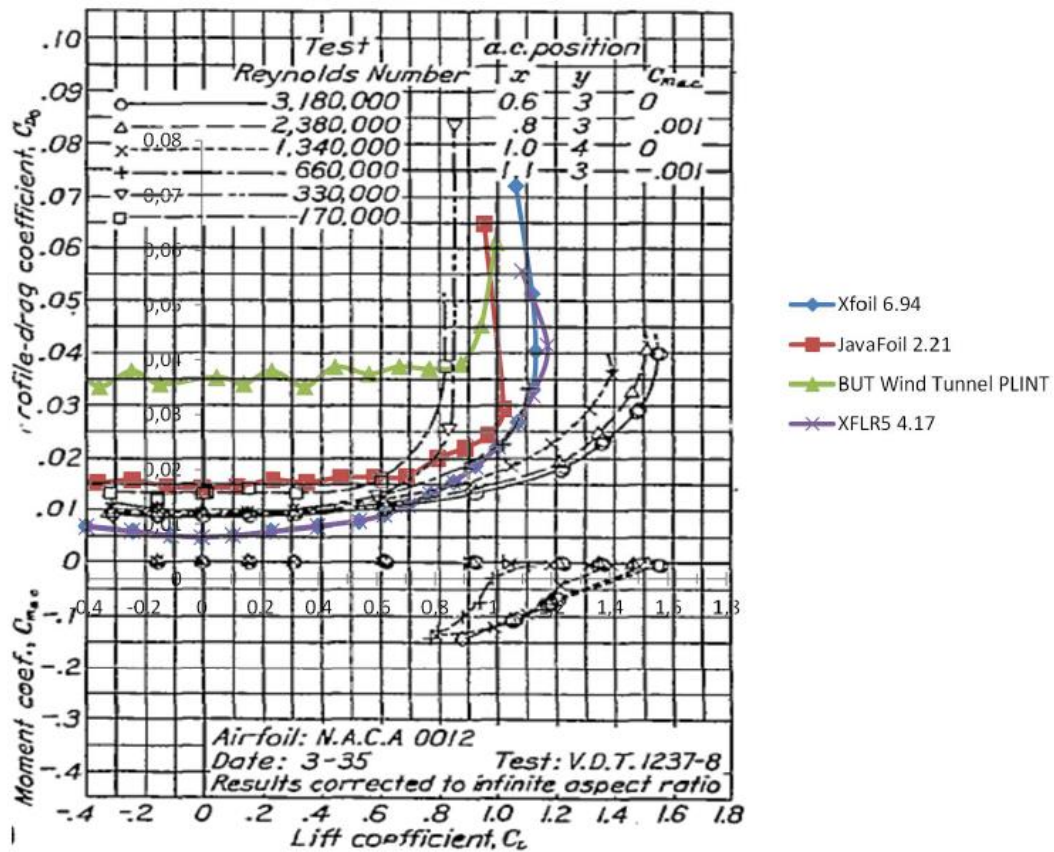


Fig. 5.6 Polar curves for NACA 0012 airfoil exported to NACA report No. 586

5.4 Evaluation of results

If it's consider NACA report as an etalon for an aerodynamic characteristics of an airfoil NACA 0012, from all three panel codes used in this thesis, JavaFoil has the most accurate results. In lift curve graph all three panel codes and wind tunnel have almost the same slope of c_l versus α curve and it was close to 2π . In pitching moment curve also JavaFoil presented the best result with its linear curve. In computation of drag coefficient, panel codes omits friction drag component which leads to lower value of drag coefficient. But also in this computation JavaFoil recorded the best result among the panel codes and its curve is closest to the one in the NACA report. XFOIL (thus also XFLR5) has the lowest value of drag coefficient in the comparison and on the other side is wind tunnel measurement with highest values of drag coefficient.

In terms of user interface, JavaFoil and XFLR5 are on the similar level. Both panel codes have a nice and user friendly workspace with many options to perform. Work with this two panel codes was quite fast and export of the results for further analysis is enabled by the program by simple pushing a button. On the other hand XFOIL has user's interface hard to work with, there is a necessity to know exact commands to perform the given tasks with at given amount of time.

CONCLUSION

This work is focused on creating the overview of the currently most used panel codes. The main task was to describe basic principles of panel method, comparison of various implementation and evaluation (accuracy, applicability) for typical tasks.

As an introduction to the problem, chapter 1 discusses the basic aerodynamic characteristics of an airfoil and explains its main geometrical variables. It gives detailed description of lift coefficient, pitching moment coefficient, drag coefficient and shows particular curves which characterize those airfoil parameters.

The main aim of this thesis was to describe panel codes, its development throughout the history and finally to use some of them and compare the results between programs. All panel codes used in this thesis are open source programs widely used between university students.

Thesis was added by wind tunnel measurement which represents the experimental method of determining the aerodynamic characteristics of an airfoil. Complete description of the measurement and test setup is in chapter 3.

NACA report served as a benchmark result for this thesis.

After investigating the panel codes and wind tunnel measurement there must be an agreement with the statement in the introduction of this thesis that man-hour and hardware requirements are incomparable between those two ways which investigates the aerodynamic characteristics of an airfoil.

BIBLIOGRAPHY

- [1] Kuethe, A., Chow, Ch.-Y., *Foundations of Aerodynamics – Bases of Aerodynamic Design*. 5th ed., John Wiley & Sons, Inc., ISBN 0-471-12919-4
- [2] Plotkin, A., Katz, J., *Low-Speed Aerodynamics (Cambridge Aerospace Series)*. 2nd ed., Cambridge University Press, ISBN 978-0521665520
- [3] Drela, M., Youngren, H., *XFOIL 6.94 User Guide* [online], 2001. Available from: <http://web.mit.edu/drela/Public/web/xfoil/>
- [4] Hepperle, M., *JavaFoil User's Guide* [online], 2014. Available from: [http://www.mh-aerotoools.de/airfoils/java/JavaFoil Users Guide.pdf](http://www.mh-aerotoools.de/airfoils/java/JavaFoil%20Users%20Guide.pdf)
- [5] *Guidelines for XFLR5 v4.16*. April 2009. Available from: <http://sourceforge.net/projects/xflr5/files/Guidelines.pdf/download>
- [6] Ballmann, J., Eppler, R., Hackbusch, W., *Panel Methods in Fluid Mechanics*. ISBN: 978-3-528-08095-2 (Print) 978-3-663-13997-3 (Online)
- [7] *Wikipedia: Aerodynamic potential flow-code* [online]. 11. April 2014 [cit. 2014-05-14]. Available from: http://en.wikipedia.org/wiki/Aerodynamic_potential-flow_code.
- [8] *Wikipedia: Computational fluid dynamics* [online]. 7. May 2014 [cit. 2014-05-14]. Available from: http://en.wikipedia.org/wiki/Computational_fluid_dynamics
- [9] Eppler, R., *Eppler airfoil design and analysis code*. [online]. Available from: <http://www.airfoils.com/eppler.pdf>
- [10] *Wikipedia: National Advisory Committee for Aeronautics* [online]. 10. February 2014 [cit. 2014-05-14]. Available from: http://en.wikipedia.org/wiki/National_Advisory_Committee_for_Aeronautics
- [11] *Wikipedia: Wake* [online]. 26. April 2014 [cit. 2014-05-28]. Available from: <http://en.wikipedia.org/wiki/Wake>

LIST OF SYMBOLS

Symbol	Unit	Value
α	[°]	Angle of attack
α_{stall}	[°]	Angle of attack at maximum lift coefficient
ρ	[kg*m ⁻³]	Density
c	[m]	Chord length
c_d	[1]	Sectional drag coefficient
C_{Df}	[1]	Friction drag coefficient
C_{Dp}	[1]	Pressure drag coefficient
c_l	[1]	Sectional lift coefficient
$c_{l\text{max}}$	[1]	Sectional lift coefficient at α_{stall}
c_{mLE}	[1]	Sectional moment coefficient
C_p	[1]	Pressure coefficient
C_{pL}	[1]	Pressure coefficient on the lower surface
C_{pU}	[1]	Pressure coefficient on the upper surface
m_0	[1]	Slope of the lift curve
M	[1]	Mach number
n	[1]	Number of panels
n_{crit}	[1]	Transition criterion
p	[Pa]	Static pressure
p_0	[Pa]	Total pressure
p_∞	[Pa]	Barometric pressure
r_0	[mm]	Radius of curvature of the surface at the leading edge
Re	[1]	Reynolds number
t_{max}	[%]	Maximum thickness of an airfoil
V	[m*s ⁻¹]	Speed of the flow
V_1	[m*s ⁻¹]	Velocity of the upstream
V_2	[m*s ⁻¹]	Velocity of the downstream (wake velocity)
V_∞	[m*s ⁻¹]	Speed of the flow far from the body
x_c	[m]	Distance of z_c behind the leading edge
x_{cp}	[m]	Location of the centre of pressure behind the leading edge
x_t	[m]	Distance of t_{max} behind the leading edge
z_c	[%]	Maximum camber of the mean camber line

LIST OF FIGURES

- Fig. 1.1.** Airfoil geometrical variables
- Fig. 1.2.** Distribution of pressure coefficient on NACA 0012 airfoil at $\alpha = 6^\circ$
- Fig. 1.3.** c_l versus α curve for symmetrical airfoil
- Fig. 1.4.** Moment about leading edge
- Fig. 1.5.** Drag of an airfoil from wake measurements
- Fig. 2.1.** Panel approximation to an airfoil
- Fig. 2.2.** XFOIL initial window
- Fig. 2.3.** XFOIL panelling parameters window
- Fig. 2.4.** XFOIL output data file with results
- Fig. 2.5.** JavaFoil Geometry card
- Fig. 2.6.** JavaFoil Polar card
- Fig. 2.7.** XFLR5 Batch Analysis window
- Fig. 2.8.** XFLR5 Pressure distribution alongside the airfoil surface
- Fig. 2.9.** XFLR5 lift curve, pitching moment curve and polar curve visualisation
- Fig. 3.1.** The wind tunnel at the Institute of Aerospace Engineering,
Brno University of Technology
- Fig. 3.2.** Position of static ports alongside the surface of an airfoil
- Fig. 3.3.** Scheme of wind tunnel test section
- Fig. 3.4.** Data file with pressures on the lower surface of the airfoil
- Fig. 3.5.** Data file with pressures on the upper surface of the airfoil
- Fig. 3.6.** Data file with other wind tunnel generated data
- Fig. 4.1.** Lift curve for NACA 0012 airfoil for various Reynolds numbers
- Fig. 4.2.** Polar curve for NACA 0012 airfoil for various Reynolds numbers
- Fig. 5.1.** Result from panel codes recorded in Microsoft Excel table
- Fig. 5.2.** Result from wind tunnel and NACA report recorded in Microsoft Excel table
- Fig. 5.3.** Lift curve of NACA 0012 airfoil. $Re = 3 \times 10^5$
- Fig. 5.4.** Pitching moment curve of NACA 0012 airfoil. $Re = 3 \times 10^5$
- Fig. 5.5.** Polar curve of NACA 0012 airfoil. $Re = 3 \times 10^5$
- Fig. 5.6** Polar curves for NACA 0012 airfoil exported to NACA report No. 586

CONTENTS OF THE ENCLOSED CD

Thesis_Bilcik.pdf An electronic version of this bachelor thesis in portable document format.

NACA Report No. 586